CARBONATE SEDIMENTOLOGY AND DIAGENESIS OF AN UPPER ORDOVICIAN SPONGE-MICROBE-CEMENT MOUND ON SOUTHAMPTON ISLAND, NUNAVUT, CANADA

Ariane Castagner

Thesis submitted to the Faculty of Science in partial fulfillment of the requirements for the M. Sc. In Earth Sciences

University of Ottawa

Ottawa, Ontario

Abstract

The Hudson Bay Basin is the largest intracratonic basin in North America, but remains a frontier area for our knowledge of its stratigraphy and sedimentology and its hydrocarbon potential. Large domal reefs (up to 10 m thick and 500 m wide) in the Upper Ordovician Red Head Rapids Formation on Southampton Island developed on the margin of this shallow-marine evaporitic basin in which physical and chemical seawater parameters were distinct from the open ocean and in which a diverse community of reef-building and dwelling metazoans was unable to flourish. The main reef facies comprise boundstone and cementstone composed of various proportions of early-calcified sponge tissues, microbial encrusters, synsedimentary cement and small colonial metazoans. The accretionary mechanisms of the Red Head Rapids reefs were mainly the result of framebuilding by early-calcified sponges and small colonial corals and binding by calcimicrobial elements for the boundstone facies, and of massive aragonitic cement precipitation near the seafloor for the cementstone facies. These Upper Ordovician reefs, in which microbialites dominate but coexist with metazoans, were more widespread in the Early Ordovician immediately prior to the Middle to Late Ordovician expansion of skeletal-dominant reefs. The Upper Ordovician reefs on Southampton Island, porous and locally bitumen impregnated, underwent early marine, near-surface and progressive burial diagenesis; reducing its primary porosity but significantly increasing its secondary porosity. They represent one of the major untested petroleum play types identified in the Hudson Bay Basin.

Résumé

Le Bassin de la Baie d'Hudson est le plus grand bassin intracratonique en Amérique du Nord, mais demeure une région toujours mal connue au niveau de sa stratigraphie et sa sédimentologie et de son potentiel en hydrocarbures. Les grands récifs en forme de dôme (jusqu'à 10 m d'épais et 500 m de largeur) dans la Formation Red Head Rapids de l'Ordovicien Supérieur sur l'île de Southampton au Nunavut se sont développés en marge de ce bassin marin évaporitique et peu profond dans lequel les paramètres physiques et chimiques étaient distincts de l'océan ouvert et une communauté peu diversifiée de constructeurs récifaux a pu prospérer. Les principaux faciès récifaux comprennent des boundstones et cementstones composés de tissus d'éponge calcifiée, d'encroûtements microbiens, de ciment synsédimentaire et de petits métazoaires coloniaux. Les mécanismes d'accrétion des récifs du Red Head Rapids étaient le résultat d'une charpente construite par les éponges précocement calcifiées et les petits métazoaires coloniaux et renforcée par différents éléments microbiens pour le faciès à boundstone et de la précipitation massive de ciment aragonitique près du fond marin pour le faciès à cementstone. Ces récifs de l'Ordovicien Supérieur, dans lequel les microbialites dominent, mais coexistent avec les métazoaires, étaient plus répandues au début de l'Ordovicien immédiatement avant que les récifs construits par les métazoaires à squelette massif dominent à l'Ordovicien Moyen et Supérieur. Les récifs de l'Ordovicien Supérieur exposés sur l'île de Southampton sont poreux et localement imprégnés de bitume. Leur paragenèse montre des phénomènes de diagenèse importants depuis leur mise en place sur le fond marin jusqu'à leur enfouissement progressif causant une réduction de leur porosité primaire, mais une augmentation importante de leur porosité secondaire. Ces récifs représentent l'un des principaux types de réservoirs pétroliers identifiés, mais non testés dans le Bassin de la Baie d'Hudson.

Acknowledgements

I would like to sincerely thank Dr. André Desrochers for his financial and academic guidance and support throughout this project. I would also like to thank Denis Lavoie for his guidance and expertise on the field and during sample analyses.

I would also like to recognize Glenn Poirier from the University of Ottawa for his help with CL analyses as well as Paul Middlestead and Wendy Abdi from the G.G. Hatch Isotope Laboratory at the University of Ottawa for their assistance with stable isotope analyses.

Finally, I would like to that the RAP (Research Affiliate Program) and the Geological Survey of Canada for funding this project.

Table of Contents

List of figures

Appendix 1

Reprint 1:

Castagner, A., Desrochers, A., Lavoie, D., 2016. An unusual sponge-microbe-synsedimentary cement framework in a Late Ordovician reef, Southampton Island (Nunavut, Canada). Canadian Journal of Earth Sciences, 53, pp. 1-8.

Chapter 1. Introduction

1.1 Introduction

Lower Paleozoic strata are well exposed on Southampton Island in Nunavut, part of the Hudson Bay Basin and one of four major intracratonic basins in North America (Zhang 2010). These undeformed carbonate-dominated strata on Southampton Island include, in ascending order, the Upper Ordovician Bad Cache Rapids and Churchill River groups and the Red Head Rapids (RHR) Formation and the Lower Silurian Severn River, Ekwan River and Attawapiskat formations (Zhang 2010). Large and resistant micritic reef buildups (up to 500 m in diameter and 10 m in height) have been reported from the top of the Upper Ordovician RHR Formation just beneath the Ordovician-Silurian boundary on Southampton Island, but their framework and internal architecture are poorly known. In addition, these buildups have been described as porous biohermal structures and identified as a potential reservoir unit in the context of an established hydrocarbon system in the Hudson Bay Basin (Zhang 2010; Lavoie et al. 2013). The main goals of this study are to describe the depositional and diagenetic features of the RHR buildups by detailed outcrop mapping, petrographic observations and geochemical analyses; to interpret paleoenvironmental conditions under which they grew; and to decipher diagenetic processes that modified their porosity during burial and subsequent exhumation.

1.2 Geological context

The Hudson Bay Basin is one of four major intracratonic basins in North America (Fig. 1); the other three are the Williston, Illinois and Michigan basins. Considerable stratigraphic differences exist between these four basins as they significantly vary in thickness and facies, suggesting that they did not experience similar burial and tectonic uplift histories. The Hudson

Bay Basin has the thinnest sedimentary succession at approximately 2.5 km. This has been attributed to a stiff lithospheric root which inhibited subsidence (Eaton and Darbyshire, 2010). However, it has the largest surface area at approximately 600,000 km^2 (Hamblin, 2008). The Hudson Bay Basin has a saucer-shaped geometry with a series of central high angle faults that divided the basin into two sub-basins since the late Silurian and Devonian. The Paleozoic strata are composed of undeformed Upper-Ordovician, Silurian and Devonian rocks with Mesozoic erosional remnants and outcrops in parts of Manitoba, Ontario, Québec and Nunavut. This succession unconformably overlies the Precambrian basement, and is surrounded by the rocks of the Precambrian Canadian Shield (Fig. 2).

Southampton Island is one of several northern islands in Nunavut on which the Paleozoic succession is exposed. The Upper Ordovician and Silurian succession is preserved on the southern and western parts of Southampton Island (Fig. 3) (Zhang 2010).

1.2.1 Tectonic history

The Hudson Bay region includes three major tectonic elements: The Paleozoic Hudson Bay Basin and a number of Archean-Paleoproterozoic domains (Eaton and Darbyshire, 2010). The Hudson Bay region was formed following the Trans-Hudson Orogen (THO) which records the collision between two cratons: the Superior craton, the largest Archean craton, and the Hearne craton. The subsidence of the Hudson Bay Basin began at roughly the same time as the Michigan Basin, possibly due to metamorphism of lower-crustal material to denser eclogite, which would have increased the flexural load (Eaton & Darbyshire, 2010). However, due to a stiff lithosphere underlying the Hudson Bay Basin, the subsidence only reached a few kilometers resulting in a much broader but shallower basin.

1.2.2 Basin evolution

The stratigraphic succession of the Hudson Bay Basin has been divided in four megasequences based on a subsidence analysis and seismic analyses interpretations (Pinet et al. 2013). These megasequences have been defined according to distinctive changes in subsidence (Fig. 4).

The first sequence of the basin evolution involves the deposition of the oldest stratal succession in shallow marine waters, possibly in a restricted extensional basin. The Bad Cache Rapids Group, Churchill River Group and RHR Formation were deposited during the first megasequence. The first unconformity in the succession, the Ordovician-Silurian boundary, is capping this megasequence and coincided with a major global sea level fall during the End-Ordovician glacial maxima.

The second megasequence overlies the Ordovician-Silurian unconformity and includes the Severn River, Ekwan River and Kenogami River formations. These formations were deposited in a tectonically active basin with a possible eastward tilt. Carbonate buildups present in these formations preferentially grew along uplifted fault-bounded blocks. This megasequence is capped by a second unconformity (Silurian-Devonian boundary) which formed either by global sea level fall or the tectonic uplift related to the Caledonian Orogeny (Pinet et al. 2013).

The third megasequence includes the Lower Devonian Stooping River and Kwataboahegan formations, at a time of active and more widespread faulting in the basin. This faulting separated the basin into two sub-basins but they eventually reconnected to form a single basin. This sequence is capped by a third unconformity representing a 4-10 Ma sedimentary hiatus (Pinet et al. 2013).

Finally, the fourth megasequence is composed of the remaining Middle and Upper Devonian Moose River, Murray Island, Williams Island and Long Rapids formations, which were deposited in a shallow marine setting.

1.3 Stratigraphy

The Upper Ordovician to Devonian stratigraphic units of the Hudson Bay Basin are primarily composed of limestones, dolomites, evaporites, sandstones and shales, which were deposited in relatively shallow marine environments (Fig. 5), but only the Upper Ordovician stratigraphy is described below.

1.3.1 Upper Ordovician Stratigraphy

The Upper Ordovician stratigraphy of the Hudson Bay Basin consists of three groups or formations; the Bad Cache Rapids Group, the Churchill River Group and the Red Head Rapids (RHR) Formation. The Upper Ordovician assemblage is bound by two major unconformities; the basal Precambrian-Phanerozoic unconformity and the Ordovician-Silurian unconformity at the top (Pinet et al. 2013). This assemblage consists of a thin basal siliciclastic unit overlain by a carbonate-dominated succession. Based on their conodont fauna (Zhang 2013), the Bad Cache Rapids Group is assigned to an Edenian-Maysvillian age while the RHR Formation is late Richmondian in age. Also, the examined Upper Ordovician succession corresponds to the litho-tectonic Tippecanoe I sub-sequence of Sloss (1988).

1.3.2 Bad Cache Rapids Group

The Bad Cache Rapids Group is the oldest unit of the Paleozoic Hudson Bay Basin succession and unconformably overlies the Precambrian basement. It is approximately 65 m

thick and is made of two main lithological units: a thin (2 m) basal siliciclastic unit overlain by a much thicker dark grey fossiliferous limestone. The middle and upper parts of the limestone unit are rich in fossil corals, gastropods, nautiloids, algae and crinoids (Zhang 2010).

1.3.3 Churchill River Group

The Churchill River Group conformably overlies the Bad Cache Rapids Group. This group ranges from 70-112 m thick in well logs and is comprised of dolostone, locally bituminous limestone and minor anhydrite (Lavoie et al. 2013).

1.3.4 Red Head Rapids Formation

The Red Head Rapids (RHR) Formation conformably overlies the Churchill River Group and is unconformably overlain by the Silurian Severn River Formation. The RHR Formation has been divided into four units by Heywood and Sanford (1976) and Zhang (2008).

The first unit, at the base of the formation, is composed of a 30 m thick laminated argillaceous dolomitic limestone interbedded with three oil shale beds. The three oil shale beds (0.4-1.0 m thick) are best exposed at Cape Donovan on northeastern Southampton Island (Zhang, 2010). The second unit is a 10-15 m thick massive breccia dolostone or limestone. The third unit is a 10 m thick massive biostromal dolostone or dolomitic limestone. Finally, the fourth and stratigraphically highest unit, which is the focus of this study, is a thin-bedded dolomitic limestone with bioherms.

1.4 Hydrocarbon system

Several critical stratigraphic elements are needed to produce a working hydrocarbon system (Magoon and Beaumont 1999). Stratigraphic critical elements are: mature source rocks,

reservoir rocks and seals and/or traps. The Hudson Bay Basin displays potential for each of these critical elements (Lavoie et al. 2015).

1.4.1 Source rocks

A potential source rock contains enough organic matter to generate and expel hydrocarbons if subjected to thermal maturation (Law, 1999). The quantity of organic matter remaining in a source rock is measured by its total organic carbon (TOC) in weight percentage; a good to excellent generation potential is typically between 2.0-5.0 Wt% TOC in shales.

The lower Paleozoic succession of the Hudson Bay Basin has several potential source rocks including the three oil shale beds present in the cyclic carbonate-evaporite unit at the base of the Red Head Rapids Formation (Zhang, 2010; Lavoie et al. 2015). Petrographic studies on the organic matter preserved in these oil shales indicate the presence of algae, chitinozoans, conodonts and graptolites. TOC values derived from Rock-Eval analyses range from 0.31% to 34.1% suggesting that the RHR oil shales have a significant hydrocarbon yield potential. Other identified source rocks in the basin include the marine black shales of the Upper Devonian Long Rapids Formation with values ranging from 2.42 wt% to 11.21 wt% TOC.

1.4.2 Reservoir rocks

Reservoir rocks are rocks that have the ability to store fluids inside their pores and in which they can be accumulated (Gluyas & Swarbrick, 2004). Thus, porosity and permeability are critical features of a potential reservoir rock in order to accumulate oil in economic quantities. Reservoir rocks in the Lower Paleozoic part of the Hudson Bay Basin are mainly represented by the large reefal structures resent in the upper RHR Formation. They have been described as porous structures with abundant centimeter-scale vugs locally filled with bitumen in the field

(Zhang 2010; Lavoie et al. 2015) and up to 15% in porosity (Hu and Dietrich, 2012). These porous structures are of particular interest due to their position stratigraphically above the three oil shale beds present in unit 1 of the RHR Formation.

In addition to those in the RHR Formation, porous reefal structures are present in the Lower Silurian Attawapiskat Formation and similar in age and in composition to the hydrocarbon productive reefs of the Guelph Formation in Southern Ontario (Lavoie et al. 2015).

1.4.3 Traps and seals

A potential seal is a unit that is impermeable and will prevent further upward migration of hydrocarbons. These seals include shales or evaporites which are present within the lower and middle Paleozoic succession of the Hudson Bay Basin. Elevated pressures in several wells, suggest that there were effective seals (Hu and Dietrich, 2012). In addition, there are several potential structural and stratigraphic traps in the lower Paleozoic part of the Hudson Bay Basin (see below).

1.5 Hydrocarbon plays

Five conventional petroleum plays have been identified in the Paleozoic strata of the Hudson Bay and Moose River basins (Lavoie et al. 2013). These five conventional play types include fault blocks, reefs, fault-bounded sags, unconformity traps and salt dissolution structure. The fault block play, which could have acted as a structural trap for hydrocarbons, was the main target of previous exploration efforts as offshore wells were focused on the tilted blocks in the center of the basin. However, this resulted in no economic discoveries.

Another potential stratigraphic structural trap involves the unconformity play which is associated with stratal truncation or onlap. As discussed above, several major unconformities are present in the basin.

Fault-controlled dolostones are significant conventional oil and gas reservoirs in other Paleozoic intracratonic basins (Michigan and Illinois basins), and are potentially present in the Hudson Bay Basin. This play involves extensional or transtensional faulting and associated sags (collapse zones). These fault zones provide a conduit for high temperature fluids which would have altered adjacent sedimentary units and may have increased local maturation levels and oil generation (Lavoie et al. 2013).

Because several evaporitic units are present in the Hudson Bay Basin, there are potential hydrocarbon plays associated with the salt dissolution or collapse. The identification of locations where there has been partial or complete removal of salt horizons could lead to the discovery of hydrocarbon pools (Halabura and Potter, 1999). Similar plays are well documented in the age-equivalent Williston Basin.

Finally, the reef play is the main focus of the current efforts in the hydrocarbon exploration of the Hudson Bay Basin. This play includes pinnacle, patch and barrier reefs occurring at several stratigraphic levels throughout the succession. The porous RHR Formation reefal structures overlying the major source beds of the basin is one of the most promising plays.

1.6 Exploration history

The exploration history of the Hudson Bay area began with Robert Bell's geological visits in the 1870's. The earliest hydrocarbon exploration of the Hudson Bay Basin began in the

1920's with intermittent drilling, followed by the first shallow wells in the 1940's (Hamblin, 2008).

The most active exploration period in the Hudson Bay area was in the 1960's to the 1980's. Following seismic surveys and drill core programs in the early 1960's, a generalized geological map for the Hudson Bay Basin was published (Sanford and Norris, 1973). These subsurface data allowed researchers to recognize the presence of up to 2000 m of Phanerozoic strata in the central part of the Hudson Bay Basin.

In total, nine wells have been drilled in the Hudson Bay Basin – four onshore and five offshore. The first onshore well was drilled in 1966 (Kaskattama No. 1), which was followed by three more in the 1970's (White Bear Creek No.1, Comeault No.1 and Pen Island No.1). Offshore drilling began in 1969 with Walrus A-71, Narwhal O-28 and Polar Bear C-11 in 1974 and ended with Beluga O-23 and Netsiq N-01 in 1985. No commercially significant discoveries have been reported from these wells, although traces of oil and gas have been reported.

1.7 Previous studies

The geological research on the Hudson Bay Basin is still in its early stages. It is the least studied of the four North American intracratonic basins due to its remote locations and limited outcrop exposures. The first geological reports of the Hudson Bay Basin only superficially explored its hydrocarbon potential (Nelson, 1694; Sanford and Norris, 1973) and produced the first geological map of the study area on Southampton Island (Heywood and Sanford 1976).

As part of the GEM programs of Natural Resources Canada starting in 2008, research activities resumed in the Hudson Bay Basin to re-evaluate its hydrocarbon resource potential using available geoscience data and the acquisition of new data (Nicolas et al. 2009). The most

recent results, including maturation levels, thermal basin history and hydrocarbon generation models, have been summarized by Lavoie and others in 2015. More specific to our study, several key Upper Ordovician geological localities on Southampton Island have been briefly described in GSC open GSC files (Zhang 2010; Lavoie 2015). Finally, the unusual composition of the Upper Ordovician RHR Formation reef framework was recently described and interpreted by the author (Castagner et al. 2016, see in appendix).

Chapter 2. Methods

2.1 Field Methods

The study area is located approximately 34 km southwest of Coral Harbour on Southampton Island (64°2’34.8”N, 83°49’33.60”W) and corresponds to locality #13 in figure 3. This locality shows a large, resistant mound at the top of the RHR Formation exhumed by recent erosion. The mound is approximately 400 m long (NW-SE direction), 250 m wide and 10 m thick (Fig. 6). In total, 87 hand samples were collected in 0.5 m vertical increments along six representative sections located around the exhumed reef core. These sections range from 2.5 m to 9 m and each section contains up to 18 samples.

2.2 Laboratory Methods

87 thin sections, one per sample, were made and stained with alizarin red S and potassium ferricyanide (Dickson 1966). These thin sections were examined under transmitted light and cathodoluminescence microscopy to identify both primary and diagenetic components present in the RHR Formation reef samples. Under the microscope, the main primary components were used to identify microfacies. A microfacies is described as the total of all sedimentological and paleontological data, which can be described and classified from thin sections, peels, polished slabs or rock samples (Flügel 2004). Microfacies are defined from information about the main components, matrix, bioclasts, primary and secondary textures to help gather information about the environment of deposition. Wright’s (1992) classification with modifiers is used in this study to name the microfacies (see appendix). This classification

differentiates between microfacies deposited through depositional, biological and diagenetic processes, including synsedimentary processes.

In addition, cathodoluminescence (CL) microscopy analyses were performed on representative thin sections of each microfacies. The CL microscopy was done on a CITL Mk5 Optical Cathodoluminescence Microscope Stage. General operating conditions were a beam energy (accelerating voltage) of 78-27 kv, beam current of 460-600 milliamps, and operating vacuum of 0.03-0.05 torr. Air was the ambient gas used in the CL chamber.

The CL microscope is a valuable and inexpensive tool in petrographic studies and provides information on the spatial distribution of trace elements and the porosity evolution in sedimentary rocks (Scholle & Ulmer-Scholle 2003). It provided critical information about diagenetic relationships between grains, matrix, cement and porosity present in the samples. Cement phases in carbonate rocks play a fundamental role in controlling porosity and permeability relationships as cement can bridge and bind grains, fill intraparticle pore space and replace earlier pre-existing carbonate phases. This can lead to complex porosity and permeability relationships, which can produce petroleum reservoirs. CL also provided information about common replacement reactions during the diagenesis of carbonate rocks. CL microscopy combined with petrographic microscopy was used to recognize the paragenetic diagenetic succession present in the studied RHR Formation reefal structures. Carbonate minerals under CL microscopy produce distinct CL zones ranging from luminescent to dully luminescent to non-luminescent (Scholle & Ulmer-Scholle 2003). Mn^{2+} may occupy either Ca^{2+} or Mg^{2+} sites, resulting, respectively, in red or yellow cathodoluminescence (Boggs and Krinsley, 2006). The amount of Mn^{2+} necessary to generate cathodoluminescence appears to depend, in part, on the presence of other activators and quenchers, the most important of the latter being Fe^{2+}. The

concentrations of both iron and manganese taken up in crystals during growth appear to be controlled by the fluctuating Eh of the formative pore waters. When departing from the oxidizing conditions present near the sediment-water interface, Mn^{2+} is first reduced and is more readily incorporated into the diagenetic carbonate minerals. Brightly luminescent zones indicate abundant Mn^{2+} in these minerals. As the levels of oxygen drop further, Fe is reduced and both elements can be incorporated into the cement. The incorporation of Fe^{2+} quenches luminescence and causes non-luminescent into the new diagenetic carbonate minerals (Boggs and Krinsley, 2006).

Primary and diagenetic components were sampled using a microdrill from 44 polished slabs for $\delta^{13}C$ and $\delta^{18}O$ analyses. These analyses were performed with a Gas Bench II interfaced with a Finnigan Mat Delta XL mass spectrometer at the G.G. Hatch Laboratory at the University of Ottawa. Data are reported as $\delta^{13}C$ and $\delta^{18}O$ in permil with respect to the Vienna Pee Dee Belemnite (VPDB) standard with an analytical precision of ±0.1‰.

Chapter 3 – Carbonate sedimentology

3.1 Field observations

The studied reef mound at the top of the RHR Formation (400 m long x 250 m wide x 10 m high) displays two main macroscopic facies in the field; stratiform and massive (Fig. 7). The stratiform facies shows poorly bedded buff weathered dolomitic limestone forming unit up to 1 m thick, while the massive facies is a massive featureless light grey limestone. The latter facies form more than 95% of the reef mound volume at the study site. The massive limestone displays a clotted, micritic fabric in which no primary components could be identified other than rare rugose and tabulate corals. Small centimeter-scale vuggy cavities are common in the massive limestone facies, either partially or completely filled with calcite spar cement. Bitumen is locally present within the cavities.

3.2 Carbonate petrology

Four main primary components grouped into three main microfacies are present in the studied RHR Fm. mound.

3.2.1 Primary components (description and interpretation)

Four primary components have been identified along the six transects located around the RHR Fm. reef mound (see tables 1-6 in appendix 1); a synsedimentary calcite spar cement, microbial components, cryptic sponge tissues and a secondary metazoan frame building assemblage.

The synsedimentary calcite spar cement is the most abundant component in the mound (Figs. 8 A and B). This cement is inclusion-rich, nonferroan, and present either as isopachous

layers of fibrous calcite or as an equigranular mosaic with curved and wavy crystal boundaries. Crystals forming botryoids are common, suggesting an original aragonitic composition for this cement (Fig. 8 C) (Davies, 1977). Square crystal terminations are locally present further supporting an original aragonitic composition (Fig. 8 D). This suggests that the inclusion-rich cement formed as the neomorphic replacement of a synsedimentary aragonitic cement. In CL microscopy, this cement has a bright orange luminescence (Fig. 9).

Second, the microbial component is commonly found encrusting other bioclasts (metazoan and sponges) (Fig. 10 A) or intergrown with the synsedimentary cement (Fig. 10 B). The microbes are present; either as peloidal laminae or centimeter-scale micritic bush-like fabrics with variously preserved *Epiphyton*- and *Renalcis*-like forms showing a preferential upwards growth pattern (Figs. 10 C and D) (Pratt & Haidl, 2008). Another, but less common, microbial form is a laminated automicrite (Fig. 11). We define this automicrite as an encrusting, peloidal and laminated micrite which is the result of microbial activity. The close spatial relationship between the various microbe forms and the sponge component (see below) suggests that the latter provided substrates for the attachment and development of microbes and calcimicrobes and allowed them to play an essential role as reef consolidator. In CL microscopy, the microbial components are non-luminescent (Fig. 12).

Third, the cryptic sponge tissues display complex centimeter-scale structure formed by inclusion-rich, nonferroan calcite crystals with a cryptic spicular network (Fig. 13). This component is also interpreted as a neomorphic replacement of an original aragonite skeleton, as evidenced by the presence of yellowish, equant, non-drusy, pseudopleochroic crystals with irregular crystal edges. The precipitation of aragonite crystals in decaying modern sponges is

well documented (Neuweiler et al. 2007). The sponge tissues are mostly dull to moderate CL luminescence with a blotchy pattern (Fig. 14).

Finally, small, centimeter-scale colonial metazoans are locally present (Fig. 15). These metazoans, mainly tabulate and rugose corals, are present in growth position and can be seen encrusted by calcimicrobes. Their skeletons are pervasively neomorphosed but key relict features (e.g. septa) are locally preserved (Figs. 15 A and B). The role played by these small colonial metazoans was somewhat minor, but their close association with *in situ* sponge tissues suggests that they were in competition as reef builders. Other invertebrates associated with these limestones are sparse including a single cephalopod, rare crinoids and ostracods (Figs. 15 C and D).

3.2.2 Microfacies - Boundstone

A boundstone is bound by *in situ* organisms during deposition (Wright, 1992). The boundstone facies is the most abundant microfacies in the studied RHR mound and is dominated by biological components – sponges, calcimicrobes and metazoans (Fig. 16). It can be divided into two end-member microfacies based on the most common reefal organisms; either sponge-dominated boundstones or coral-dominated boundstones. This microfacies is present in 50 of our 87 samples (57%) and occurs in all studied sections.

3.2.3 Microfacies – Cementstone

A cementstone is defined as a limestone which is mainly composed of calcite spar cement (commonly replaced or recrystallized) in which grains or *in situ* organisms do not constitute a framework (Wright, 1992). The cementstones in the studied RHR Fm. mound are present in all measured sections and composed of synsedimentary inclusion-rich calcite spar cement (Fig. 17

A). However, other components are present, particularly *Epiphyton*- and *Renalcis*-like calcimicrobes intergrown with the synsedimentary calcite cement (Fig. 17 B). This microfacies is present in 28 of our 87 samples (32%).

3.2.4 Microfacies – Rudstone

The third and last microfacies is a rudstone. A rudstone is defined as grain-supported with grains (intraclasts) greater than 2 mm (Wright, 1992). The intraclasts in this microfacies are angular, approximately 500 μm to 2.5 mm in size, composed mainly of cementstone and commonly cemented together by isopachous layers of the synsedimentary calcite spar cement (Fig. 18). This microfacies is present only in four of our samples (5%).

3.2.5 Depositional interpretation

Any interpretation of the depositional environment of the RHR Formation mound must meet the following conditions; 1) a limited epifaunal biota associated with abundant sponges and calcimicrobes and to a lesser extent tabulate corals; 2) a sparse occurrence of depositional lime mud within the RHR mound; and 3) abundant aragonitic precipitation as synsedimentary precipitates near the seafloor or as early replacement in decaying sponges.

The studied RHR Fm. mound developed in a restricted, hypersaline basin following the late Ordovician glacioeustatic sea-level fall and the development of the Ordovician-Silurian unconformity within the Hudson Bay Basin (Lavoie et al. 2013). This regression resulted in conditions of restricted basin circulation and increased evaporation, as evidenced by the presence of coeval precipitation of subaqueous evaporites in the subsurface of the central Hudson Bay Basin (Hu et al. 2011). This hypersaline environment was unfavorable for open marine stenohaline taxa (James and Jones 2015); thus explaining the low diversity present in the RHR

Fm. reef. On the other hand, sponges and microbes were ideally adapted to survive under such extreme environmental conditions (Scholle & Ulmer-Scholle, 2003).

3.3 Carbonate diagenesis (description and interpretation)

3.3.1 Mineral phases

Diagenetic products in the studied mound include abundant inclusion-rich calcite spar cement (see above), various neomorphosed synsedimentary components (see above), common cm-scale dissolution vugs, inclusion-poor calcite spar cement, dolomite and dedolomite. The cm-scale dissolution vugs are common, interconnected and crosscut all primary components (Figs. 19 A and B). These irregular vugs locally coated with bitumen (Fig. 19 C) are either partially or completely filled with an inclusion-poor calcite cement (Fig. 19 D). This late spar cement is clear, drusy, luminescent and post-dates the inclusion-rich synsedimentary calcite spar cement in large primary pores. Dolomite and dedolomite are only locally present as small isolated millimetric dolomite rhombohedrons either completely dissolved or partially filled with calcite; thus creating additional pore space (Fig. 20).

3.3.2 Porosity

The primary growth porosity in the studied RHR Formation mound was relatively high, but pervasively and early filled by the early diagenetic, inclusion-rich calcite spar cement. A significant secondary porosity was, however, created by the formation of mm- to cm-scale dissolution vugs. The vuggy porosity is visually estimated at 5-30% in the field, but more accurately calculated at 7-15% from representative scanned thin-sections (Figs. 21 and 22).

Vertical fractures are also common, but their detailed study was beyond the scope of the present study. A secondary microcrystalline porosity associated with a dedolomitization event is present in the RHR Fm. mound, but remains relatively minor.

3.3.3 Stable isotope geochemistry

Table 7 summarizes $\delta^{13}C$ and $\delta^{18}O$ analyses of the main primary components present in the studied RHR Formation mound, and includes: the microbial component ($\delta^{13}C$ ranging from -0.22 ‰ to +3.9 ‰ and $\delta^{18}O$ ranging from -11.06 ‰ to -3.19 ‰), the neomorphosed spongial tissues ($\delta^{13}C$ ranging from 2.14 ‰ to 3.12 ‰ and $\delta^{18}O$ ranging from -7.98 ‰ and -3.63 ‰), and the synsedimentary calcite spar cement ($\delta^{13}C$ ranging from 0.45 ‰ to 2.92 ‰ and $\delta^{18}O$ ranging from -9.51 ‰ and -5.99 ‰). Other components include the inclusion-poor, calcite spar cement ($\delta^{13}C$ ranging from -2.14 ‰ to 3 ‰ and $\delta^{18}O$ ranging from -12.34 ‰ and -2.99 ‰) and the inclusion-rich synsedimentary cement intraclasts in the rudstone microfacies ($\delta^{13}C$ ranging from 0.94 ‰ to 2.87 ‰ and $\delta^{18}O$ ranging from -10.5 ‰ and -7.05 ‰). In addition, a $\delta^{13}C$ chemostratigraphic study was performed on samples of the section #6; one of the thickest sections around the studied RHR Fm. mound. The ubiquitous presence of, at least, a single primary component (synsedimentary cement, sponges, calcimicrobes) in all the section samples allowed us to produce a continuous $\delta^{13}C$ curve in which values remain relatively stable (Fig. 23). The local negative excursion may be due to subaerial exposure, which would have subjected the marine facies to erosion and meteoric waters.

The primary components of the RHR Formation reefs have similar $\delta^{13}C$ values while their $\delta^{18}O$ values are more variable. $\delta^{13}C$ values are typically less affected by diagenetic changes than $\delta^{18}O$ values, due to the fact that the system is often more or less rock-buffered for carbon

and that the pore fluids contain relatively little carbon, and are thus unable to change the isotopic composition of the rock (Banner and Hanson 1990).

A cross plot between the $\delta^{13}C$ and $\delta^{18}O$ results (Fig. 24) shows a positive standard burial trend and meteoric diagenesis (Choquette, 1990; James & Jones 2015).

3.3.4 Paragenetic sequence

The paragenetic sequence of the RHR Formation mound comprises ten distinct events that can be grouped into five diagenetic phases (Fig. 25).

The first phase (marine diagenesis) represented by the growth of the primary components present in the RHR Fm. mound. This involves the growth of sponge tissues s and colonial corals as reef framebuilders, and the various microbial components, and the massive synsedimentary aragonitic cement as important reef consolidators. The latter was a major diagenetic event filling most of the primary porosity created by reef builder organisms. Minor micritic envelopes around reef dweller skeletal debris also formed on the sea floor.

Phases 2 and 3 (meteoric and shallow burial diagenesis respectively) involve the neomorphic replacment of the reefal primary components (mainly the sponge tissues) and synsedimentary cement from aragonite to low-Mg calcite under meteoric conditions following the extensive interval of subaerial exposure at the end of the Ordovician. This neomorphic replacement most likely occurred within an active freshwater recharge zone in which fluids could actively circulate, possibly associated with the major End-Ordovician basin-scale unconformity. The pervasive neomorphic replacement here suggests that phreatic rather than vadose conditions were predominant (Pingitore, 1976). The end result was that the primary components such as sponge tissues or synsedimentary cement are difficult to recognize in thin-

sections because their microstructures are obliterated. Post-dating the neomorphic replacement, abundant mm- to cm-scale dissolution vugs formed. This dissolution event was the main enhancing-porosity process in the RHR Fm. mound because the vugs are mainly unfilled by the later cement phases. In short, the dissolution vugs occurred early because they crosscut all the primary depositional and diagenetic components present in the RHR Fm. mound. The final diagenetic event associated with this phase comprises the non-ferroan, inclusion-poor, and dully-luminescent spar cement suggesting that precipitation occurred under near surface meteoric to shallow burial conditions. A non-ferroan, inclusion-poor syntaxial spar cement is also present on rare crinoid and ostracods skeletal debris.

The fourth phase (intermediate to deep burial diagenesis) includes minor replacement dolomitization resulting in local development of ferroan dolomite crystals. This phase also coincided with the emplacement of liquid hydrocarbons in the system as evidenced by their preservation as solid bitumen coating the open dissolution vugs. Minor stylolitization also formed resulting from chemical compaction at greater burial depth.

Finally, the last phase (uplift) involves minor dedolomitization. The near-surface conditions would have resulted in dedolomitization of the ferroan dolomite crystals in the presence of fluids, which had a high Ca+/Mg+ ratio (Evamy, 1967). This process began with a selective replacement of the dolomite cores into calcite, which preserved their overall crystal shape but was subsequently dissolved. Alternatively, the dolomite may have been selectively dissolved without calcitization.

Chapter 4. Discussion

4.1 Age of the Red Head Rapids Formation

A conodont study by Zhang (2013) gave the RHR Formation a tentative Late Richmondian age due to the presence of *R. symmetricus*. However, whether this reef is Katian or Hirnantian in age, our $\delta^{13}C$ and $\delta^{18}O$ values are clearly enriched when compared to values for global marine calcite during the Katian based on a study of well-preserved brachiopods by Shields in 2003 (Fig. 24). This significant enrichment relative to Katian open ocean water may have resulted from the restricted nature of the Hudson Bay Basin in the late Ordovician. The primary productivity of the calcimicrobes within this restricted basin could have encriched the $\delta^{13}C$ values compared to typical open ocean water values, whereas the enriched $\delta^{18}O$ values may be due to increased evaporation rates (Holmden et al. 1998, James & Jones 2015). Another possibility is that these enriched values could have preserved a Hirnantian seawater signature because they occur within the range defined by well-preserved Hirnantian brachiopods (Shields et al. 2003) and, if true, the RHR Fm. may be Gamachian in age. Similar enriched $\delta^{13}C$ values have been found in the southern Hudson Bay Basin and Moose River Basin (Demski et al. 2016; Turner and Armstrong, 2015). These values have been used to claim that the Hirnantian deposition was more widespread on Laurentia than previously thought. Further coupled chemostratigraphic and biostratigraphic studies are needed to further evaluate the age of this formation.

4.2 Ordovician reefs

A basin-scale unconformity, controlled by a global End-Ordovician glacioeustatic sea-level regression, caps the RHR Formation mounds in the Hudson Bay Basin (Pinet et al. 2013).

This sea-level fall resulted in restricted basin circulation and precipitation of the basin center subaqueous evaporites (Hu et al. 2011). During the End-Ordovician the Hudson Bay Basin, which was located at within 10° of the paleoequator (Jin et al. 2013), was a region of sedimentation under evaporative conditions. Prior to their subaerial exposure, the RHR Formation buildups, occupying a basin margin position, grew in an overall hot and arid climate and isolated from the open ocean to the northeast (Sanford 1987). This shallow-marine evaporative epicratonic setting was unfavourable for most marine biota, which can only tolerate seawater of 30‰–40‰ salinity (James and Jones 2015), thus explaining the near absence of a diverse community of invertebrates and calcareous algae as reef dwellers.

The assemblage of reef-building organisms present in the RHR reef mound fundamentally differs from other shallow-water Hirnantian or late Katian reefs (Webby 2002). Reefs during the Late Ordovician are typically diverse following the Great Ordovician Biodiversification Event (GOBE) which followed the Cambrian Explosion and resulted in an important increase of marine biodiversity over approximately 25 Ma (Servais et al. 2009) (Fig. 26). This increase in diversity of species is thought to have been caused by a number of intrinsic and extrinsic factors (Harper et al. 2015). Therefore, reefs in the Late Ordovician are typically dominated by corals (namely *Tetradium sp.*), stromatoporoids or bryozoan with sponges, microbes and algae (Webby, 2002).

In contrast, Early-Ordovician reefs were mainly microbially dominated, thrombolitic and associated with some metazoan or algae due to recovery from the Cambrian crises (Webby, 2002). In the latter part of the Early-Ordovician, the first large metazoans were becoming established as frame building components. These reefs have more in common with the reefal mounds in the RHR Formation than typical Late-Ordovician reefs. Rare crinoids are also present

in the RHR mound indicating a temporary reduction in salinity within the basin, possibly due to a marine transgression or rainfall events.

4.3 Potential as a hydrocarbon reservoir

A good potential hydrocarbon reservoir is a rock body that is porous, permeable and able to store commercial amounts of hydrocarbons. Reefs are generally considered good potential reservoirs due to their abundant porosity and permeability forming about half of the world's oil and gas held in carbonates (Ahr, 2008). The porosity and permeability in carbonate reservoirs depend on the rock properties, diagenetic episodes and fracture patterns.

The primary porosity left in the RHR Fm. reef is rare to nearly absent now following neomorphism as the recrystallization of aragonite can produce closer-fitting crystal mosaics that have a lower porosity and permeability than their precursor (Ahr 2008). However, secondary porosity can be seen in this reef in the form of vugs, fractures and pores due to dedolomitization. The measured porosity within this mound is approximately between 7-15%. Since the available porosity within this reefal mound is primarily secondary porosity, this formation can be classified as a diagenetic reservoir (Ahr 2008). However, further studies would need to be performed in order to measure the mound's permeability to better characterize its reservoir potential (see below).

4.4 Conclusions

Several conclusions can be made following this study:

1) The Upper Ordovician reef buildup exposed at the top of the RHR Formation on Southampton Island, Nunavut, Canada, developed on the margin of a shallow-marine

evaporitic epicratonic basin in which physical and chemical seawater parameters were distinct from the open ocean and in which a diverse community of reef-building and dwelling metazoans was unable to flourish.

2) The massive RHR Formation mound is primarily composed of boundstone, cementstone and rudstone microfacies with various proportions of early calcified sponge tissues, microbial encrusters, synsedimentary cement and small colonial metazoans.
3) The accretionary mechanisms of the RHR Formation were mainly the result of frame-building by early calcified sponges and small colonial corals and binding by calcimicrobial elements for the boundstone facies, and of marine cement precipitation near the seafloor for the cementstone facies.
4) The RHR Formation mounds have a biotic composition more in common with the sponge-microbial reefs which dominated worldwide in the Early Ordovician. Environmental conditions, if the hypersalinity is correct, has promoted the sustained development of a biological motif of microbial and sponge-dominated reefs through time.
5) The RHR Formation mound underwent both near-surface and burial diagenesis, reducing primary porosity but increasing secondary porosity.
6) The RHR Formation mounds may be classified as a good potential diagenetic reservoir with a measured porosity between approximately 7-15%. Further studies need to be done to better decipher the potential role played by these mounds in the overall hydrocarbon system of the Hudson Bay Basin.

4.6 Further work

Further studies should be done to decipher the diagenetic environments associated with the events recognized in the paragenetic succession proposed above, including fluid inclusions and clumped isotopes. Information derived from fluid inclusion microthermometry will help to constrain the diagenetic environments of precipitation of carbonate phases as well as to obtain an estimate of temperatures of entrapment and salinities of parental fluids (Goldstein 2001). Coupled with a fluid inclusion study, clumped isotopes, a relative new but promising technique in stable isotope geochemistry, will also help to define the behavior of the temperature and $\delta^{18}O$ of these parental fluids (Eiler 2007).

References

Ahr, W. M., 2008. Geology of Carbonate Reservoirs. Wiley, ISBN 978-0-470-16491-4.

Banner, J.L., and Hanson, G.N. 1990. Calculation of simultaneous isotopic and trace element variations during water-rock interaction with applications to carbonate diagenesis. Geochimica et Cosmochimica Acta, 54, 3123–3137.

Boggs, S. Jr. and Krinsley, D., 2006. Applications of Cathodoluminescence Imaging to the Study of Sedimentary Rocks. Cambridge, New York, Melbourne: Cambridge University Press, 165 p.

Castagner, A., Desrochers, A. and Lavoie, D., 2016. An unusual sponge-microbe-synsedimentary cement framework in a Late Ordovician reef, Southampton Island (Nunavut, Canada). Canadian Journal of Earth Sciences, 53, 1-8.

Choquette, P.W. and James, N.P., 1990. Limestone: The burial diagenetic environment. In: McIlreath I. and Morrow D. (eds) *Diagenesis*. St John's, ND, Canada: Geological Association of Canada, Reprint Series 4, 75-111.

Davies, G.R., 1977. Former magnesian calcite and aragonite submarine cements in upper Paleozoic reefs of the Canadian Arctic: A summary. Geology, 5, 11-15.

Dickson, J.A.D. 1966. Carbonate identification and genesis as revealed by staining. Journal of Sedimentary Petrology, 36, 491–505.

Demski, M.W., Wheadon, B., Stewart, L.A., Elias, R.J., Young, G.A., Nowlan, G.S., and Dobrzanski, E. 2015. Hirnantian strata identified in major intracratonic basins of central North America: implications for uppermost Ordovician stratigraphy. Canadian Journal of Earth Sciences, 52, 68–76.

Eaton, D.W. and Darbyshire, F., 2010. Lithospheric architecture and tectonic evolution of the Hudson Bay region. Tectonophysics, 480, 1-22.

Eiler, J.M., 2007. "Clumped-isotope" geochemistry - The study of naturally-occurring, multiply-substituted isotopologues. Earth and Planetary Science Letters, 262, 309-327.

Evamy, B.D., 1967. Dedolomitization and the development of rhombohedral pores in limestone. Journal of Sedimentary Petrology, 37, 1204-1215.

Flügel, E., Microfacies of Carbonate Rocks, 2010. Berlin: Springer, 984 p.

Gluyas, J., and Swarbrick, R., 2004. Petroleum Geoscience, Blackwell Science Ltd, 376 p.

Goldstein, R.H., 2001. Fluid inclusions in sedimentary and diagenetic systems. Lithos, 55, 159-193.

Halabura, S. P. and Potter, D., 1999 : Salt Dissolution and Collapse : One Key to Western Canadian Oil and Gas Plays. Digging Deeper, Finding a Better Bottom Line, CSPG and the Petroleum Society of CIM Joint Conference, 82-84.

Hamblin, A.P., 2008: Hydrocarbon potential of the Paleozoic succession of Hudson Bay Bay/James Bay: Preliminary conceptual synthesis of background data. Geological Survey of Canada, Open File 5731, 12p.

Harper, D.A.T., Zhang, R-B and Jin, J., 2015: The Great Biodiversification Event: Reviewing two decades of research on diversity's big bang illustrated by mainly brachiopod data. Palaeoworld, 24, 75-85.

Heywood, W. W., and B. V. Sanford, 1976, Geology of Southampton, Coats, and Mansel Islands, District of Keewatin, Northwest Territories: Memoir 382, Geological Survey of Canada, 35 p.

Holmden, C., Creaser, R.A., Muehlenbachs, K., Leslie, S.A., Bergström, S.M., 1998. Isotopic evidence for geochemical decoupling between ancient epeiric seas and bordering oceans: Implications for secular curves. Geology, 26, 567-570.

Hu, K., Dietrich, J., Dewing, K., Zhang, S., Asselin, E., Pinet, N., and Lavoie, D. 2011. Stratigraphic correlations for five offshore wells in the Hudson Bay Basin, Northern Canada. Geological Survey of Canada, Open File 7031, 1 p.

Hu, K. and Dietrich, J., 2012. Hydrocarbon reservoir potential in Paleozoic strata in the Hudson Bay Basin, northern Canada. Geological Survey of Canada, Open File 7052, 36 p.

James, N.P., and Jones, B. 2015. Origin of carbonate sedimentary rocks. Wiley, Oxford, UK. 464 p.

Jin, J., Harper, D.A.T., Cocks, L.R.M., McCausland, P.J.A., Rasmussen, C.M.Ø., and Sheehan, P.M. 2013. Precisely locating the Ordovician equator in Laurentia. Geology, **41**: 107–110. doi:10.1130/G33688.1.

Lavoie, D., Pinet, N., Dietrich, J. and Chen, Z., 2015. The Paleozoic Hudson Bay Basin in northern Canada: New insights into hydrocarbon potential of a frontier intracratonic basin. AAPG Bulletin, 99, 859-888.

Lavoie, D., Pinet, N., Dietrich, J., Zhang, S., Hu, K., Asselin, E., Chen, Z., Bertrand, R., Galloway, J., Decker, V., Budkewitsch, P., Armstrong, D., Nicolas, M., Reyes, J., Kohn, B.P., Duchesne, M.J., Brake, V., Keating, P., Craven, J., and Roberts, B., 2013. Geological framework, basin evolution, hydrocarbon system data and conceptual

hydrocarbon plays for the Hudson Bay and Foxe basins, Canadian Arctic; Geological Survey of Canada, Open File 7363, 210 p.

Law, C.A., 1999: Treatise of Petroleum Geology / Handbook of Petroleum Geology: Exploring for Oil and Gas Traps. Chapter 6: Evaluating Source Rocks.

Magoon, L.B. and Beaumont, E.A., 1999: Treatise of Petroleum Geology / Handbook of Petroleum Geology: Exploring for Oil and Gas Traps. Chapter 3: Petroleum Systems.

Nelson, S. J., 1964, Ordovician stratigraphy of northern Hudson Bay lowland, Manitoba: Geological Survey of Canada Bulletin 108, 36 p.

Neuweiler, F., Daoust, I., Bourque, P-A and Burdige, D.J., 2007: Degradative Calcification of a Modern Siliceous Sponge from the Great Bahama Bank, The Bahamas: A Guide for Interpretation of Ancient Sponge-Bearing Limestones. Journal of Sedimentary Research, 77, 552-563.

Nicolas, M. P. B. and Lavoie, D. 2009: Hudson Bay and Foxe Basins Project: introduction to the Geo-mapping for Energy and Minerals, GEM–Energy initiative, northeastern Manitoba (parts of NTS 54); in Report of Activities 2009, Manitoba Innovation, Energy and Mines, Manitoba Geological Survey, 160–164.

Pinet, N., Lavoie, D., Dietrich, J. Hu, K. and Keating, P. 2013: Architecture and subsidence history of the intracratonic Hudson Bay Basin, northern Canada. Earth-Science Reviews 125, 1-23.

Pingitore, N. E., 1976. Vadose and phreatic diagenesis; processes, products and their recognition in corals. Journal of Sedimentary Research, 46, 985-1006.

Pratt, B.R., Haidl, F.M., 2008. Microbial patch reefs in Upper Ordovician Red River strata, Williston Basin, Sasakatchewan: Signal of heating in a deteriorating epeiric sea. Geological Association of Canada, Special Paper 48: Dynamics of Epeiric Seas.

Sanford, B. V., and A. W. Norris, 1973, The Hudson platform - Their geology and potential, R. G. McCrossan, ed., Future petroleum provinces of Canada: Memoir 1, Canadian Society of Petroleum Geologists, 387–409.

Scholle, P. A., Ulmer-Scholle, D.S., 2003. A Color Guide to the Petrography of Carbonate Rocks: Grains, textures, porosity, diagenesis. AAPG Memoir 77, American Association of Petroleum Geologists, 474 p.

Servais, T., Harper, D., Li, J., Munnecke, A., Owen, A.W. and Sheehan, P.M., 2009. Understanding the Great Ordovician Biodiversification Event (GOBE): Influences of paleogeography, paleoclimate, or paleoecology? GSA Today, 19, 4-10.

Shields, G. A., Carden, G.A., Veizer, J., Meidla, T., Rong, J.-Y., and Li, R.-Y., 2003. Sr, C, and O isotope geochemistry of Ordovician brachiopods: a major isotopic event around the Middle-Late Ordovician transition. Geochimica et Cosmochimica Acta, 67, 2005-2025.

Sloss, L. L., 1988, Tectonic evolution of the craton in Phanerozoic time, in L. L. Sloss, ed., Sedimentary cover — North America craton, U.S.: The geology of North America: Geological Society of America, D2, 25–51.

Turner, E.C., and Armstrong, D.K., 2015. Upper Ordovician stratigraphy of northern Ontario: differential subsidence and deposition in two late Ordovician basins contemporaneous with Hirnantian glaciation and the Taconic orogeny. Ontario Geological Survey Open File Report, 6313.

Webby, B.D., 2002. Patterns of Ordovician Reef Development. SEPM Special Publication No. 72, 129-179.

Wright, V.P. (1992) A revised classification of limestones, Sedimentary Geology, 76, 177-185.

Zhang, S. 2008: New insights into Ordovician oil shales in Hudson Bay Basin: their number, stratigraphic position, and petroleum potential. Bulletin of Canadian Petroleum Geology, 56, 300-324.

Zhang, S. 2013. Ordovician conodont biostratigraphy and redefinition of the age of lithostratigraphic units on northeastern Melville Peninsula, Nunavut. Canadian Journal of Earth Sciences, 50, 808-825.

Zhang, S. 2010: Upper Ordovician Stratigraphy and Oil Shales on Southampton Island Field Trip Guidebook. GSC Open File 6668, 42p.

Figures

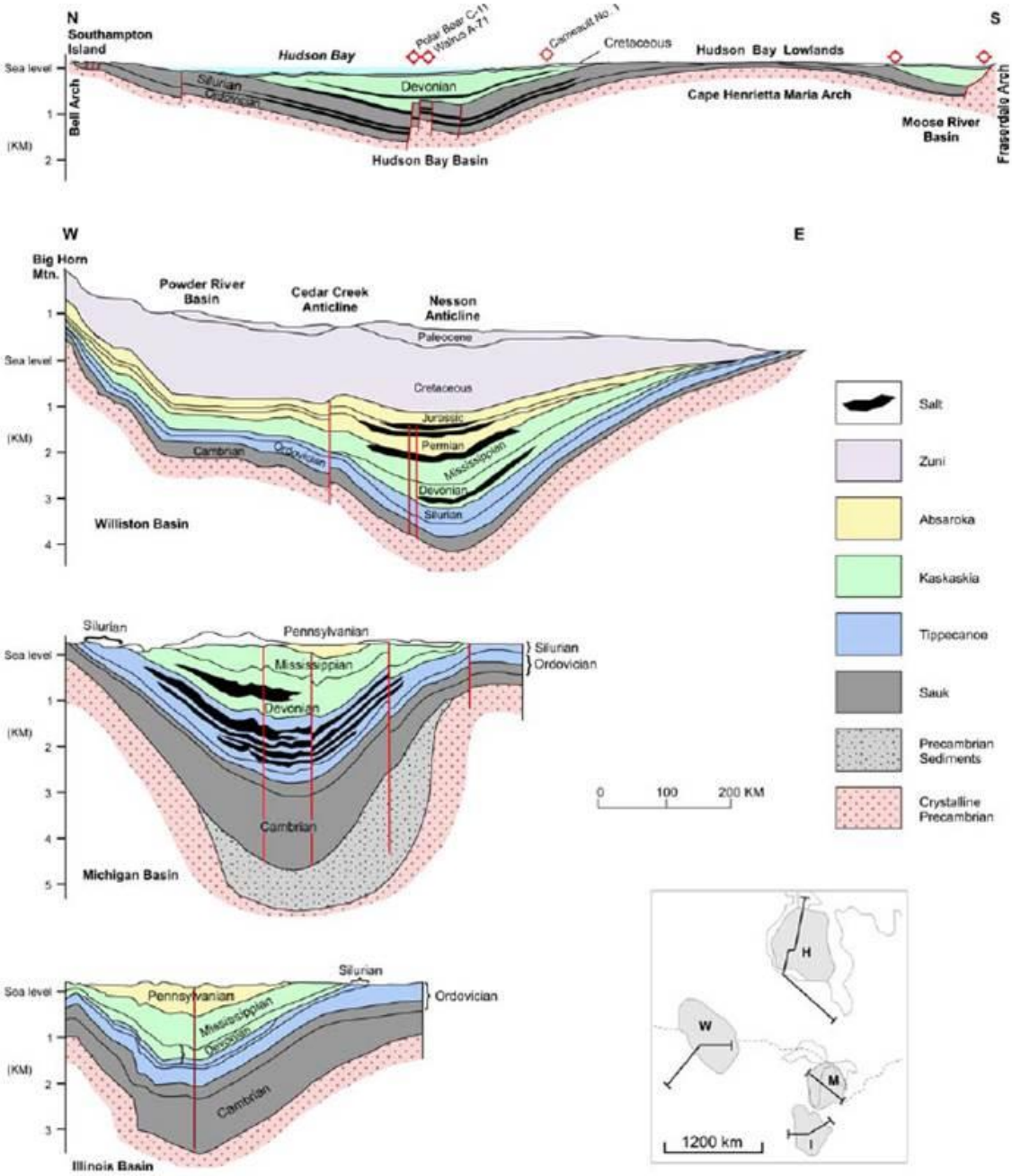

Figure 1: Schematic cross section of the four intracratonic basins in North America. Zhang (2010).

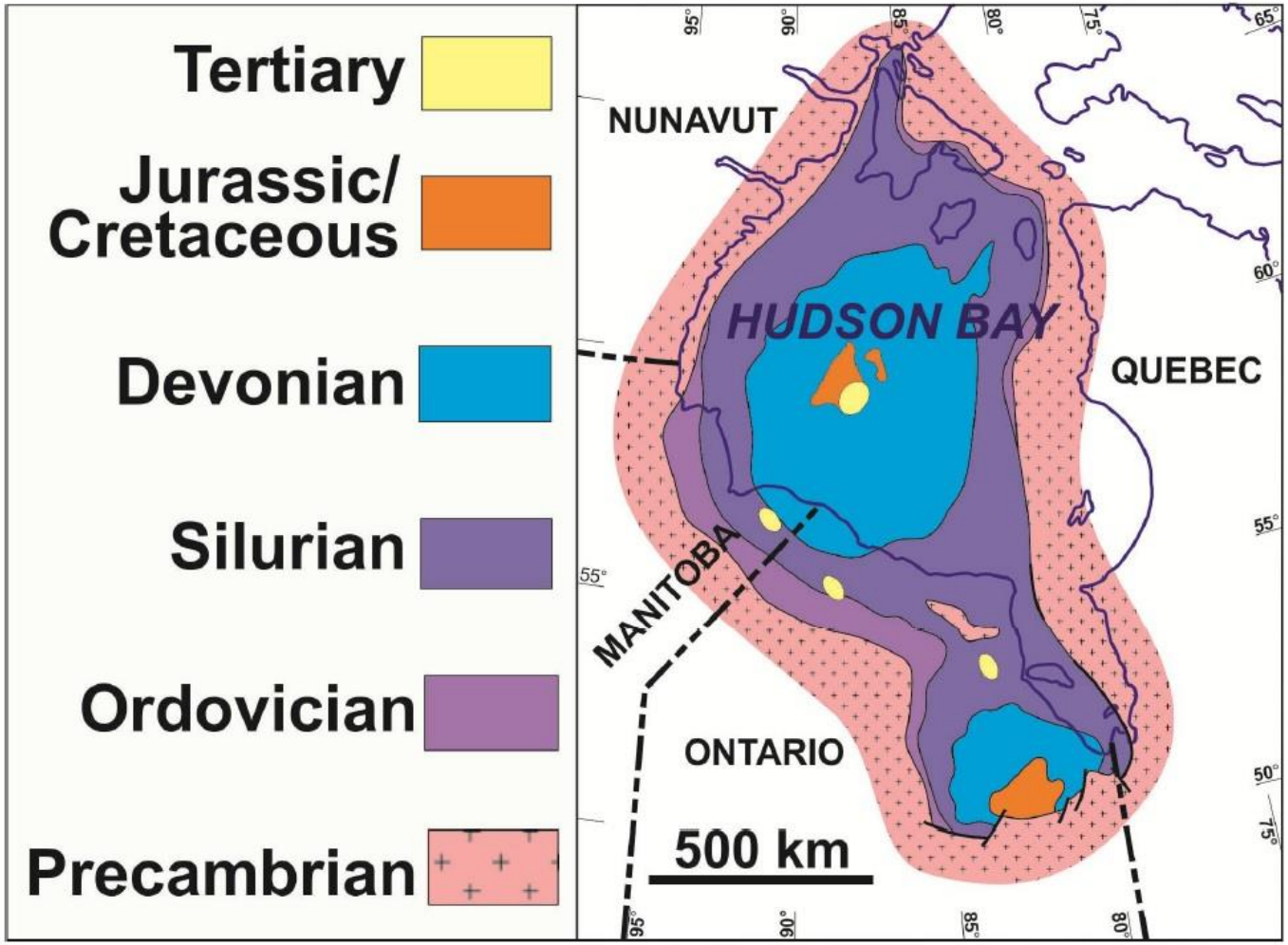

Figure 2: Simplified geological map of the Hudson Bay and Moose River basins (Lavoie 2013, modified from Hamblin 2008)

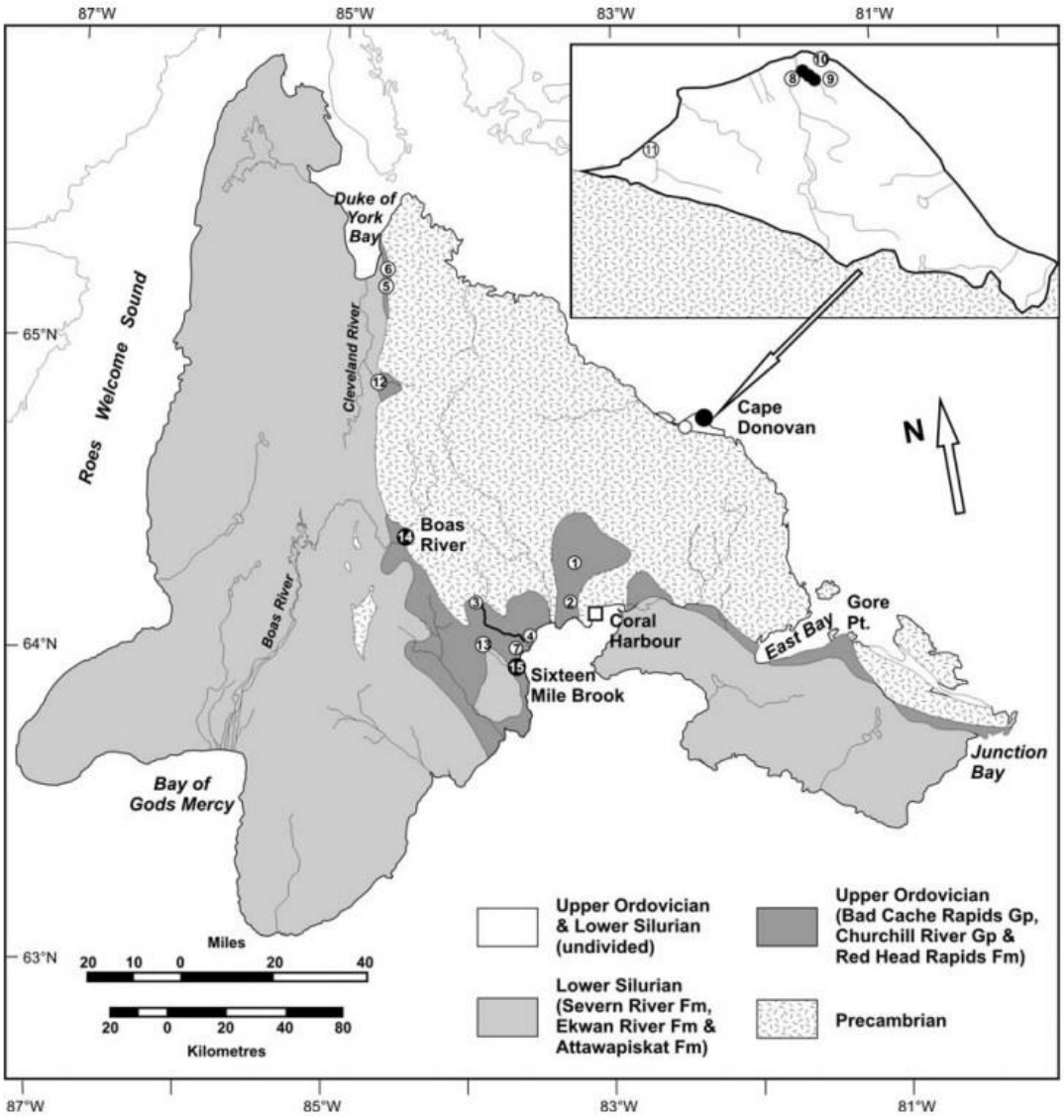

Figure 3: Simplified geological map of Southampton Island, Nunavut, Canada with numbers corresponding to localities in Zhang (2010).

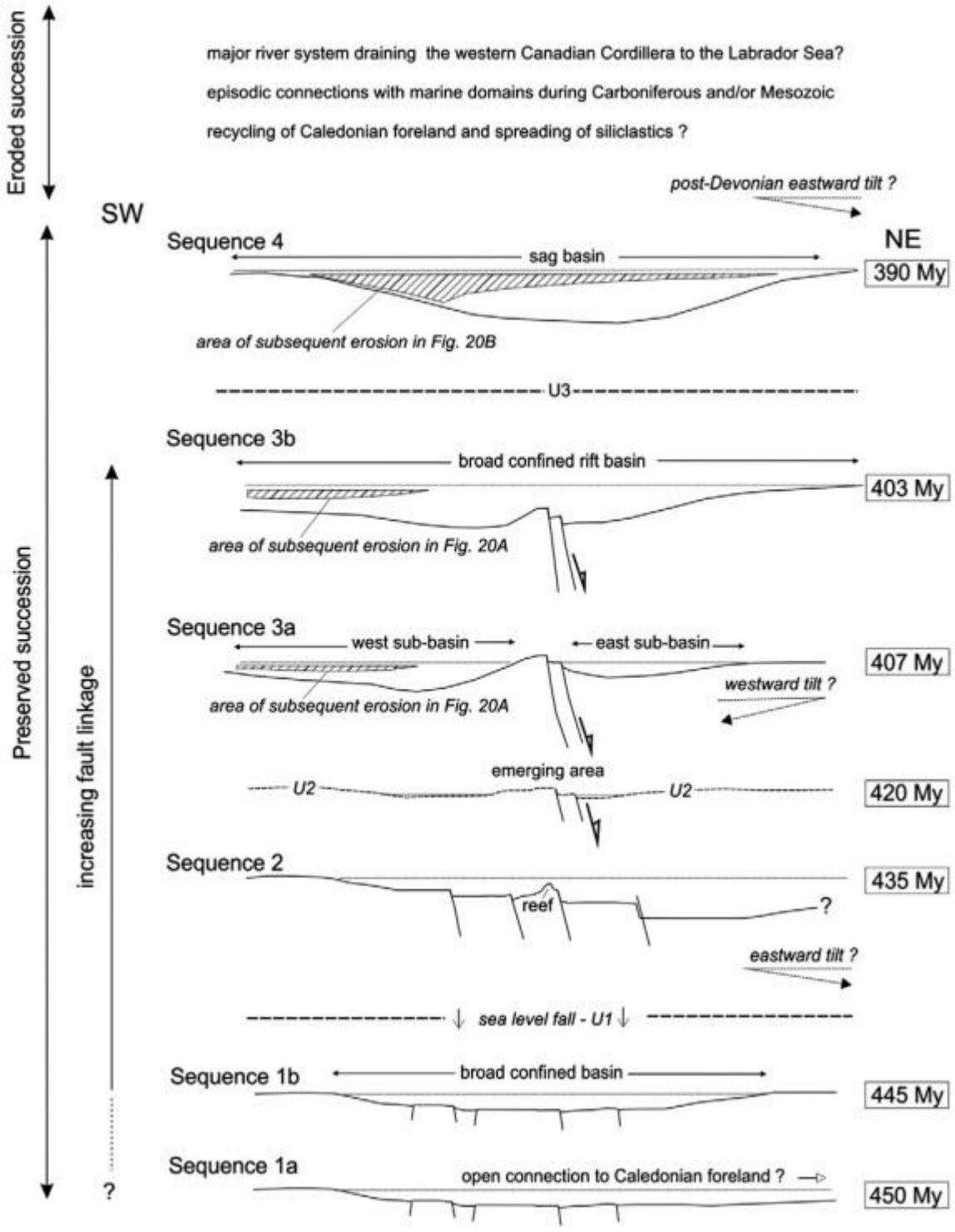

Figure 4: Schematic depositional settings of the four megasequences in the Hudson Bay Basin (Pinet et al. 2013).

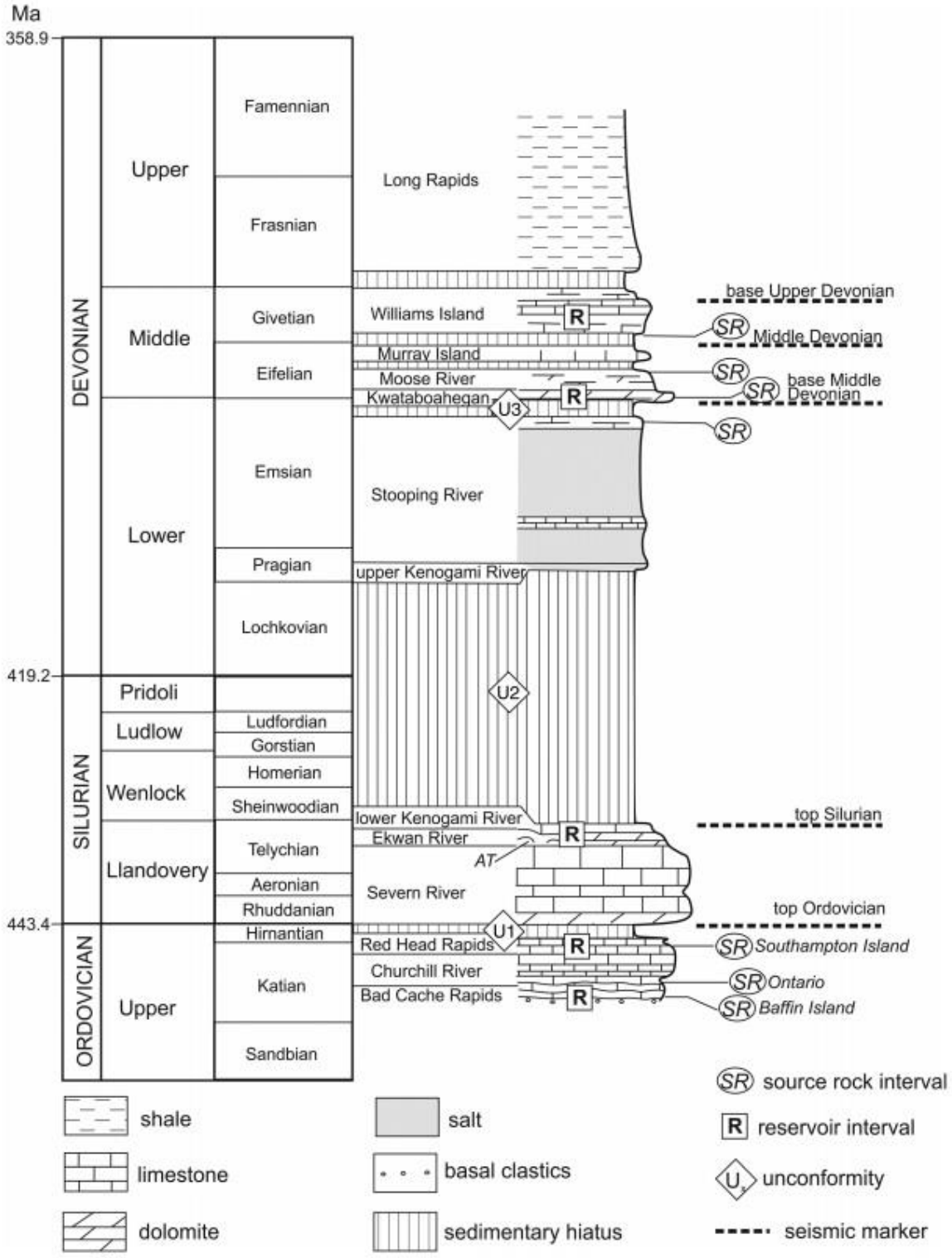

Figure 5: Paleozoic stratigraphic succession of the Hudson Bay Basin with major unconformities and potential source rock and reservoir rock intervals (Lavoie et al. 2015)

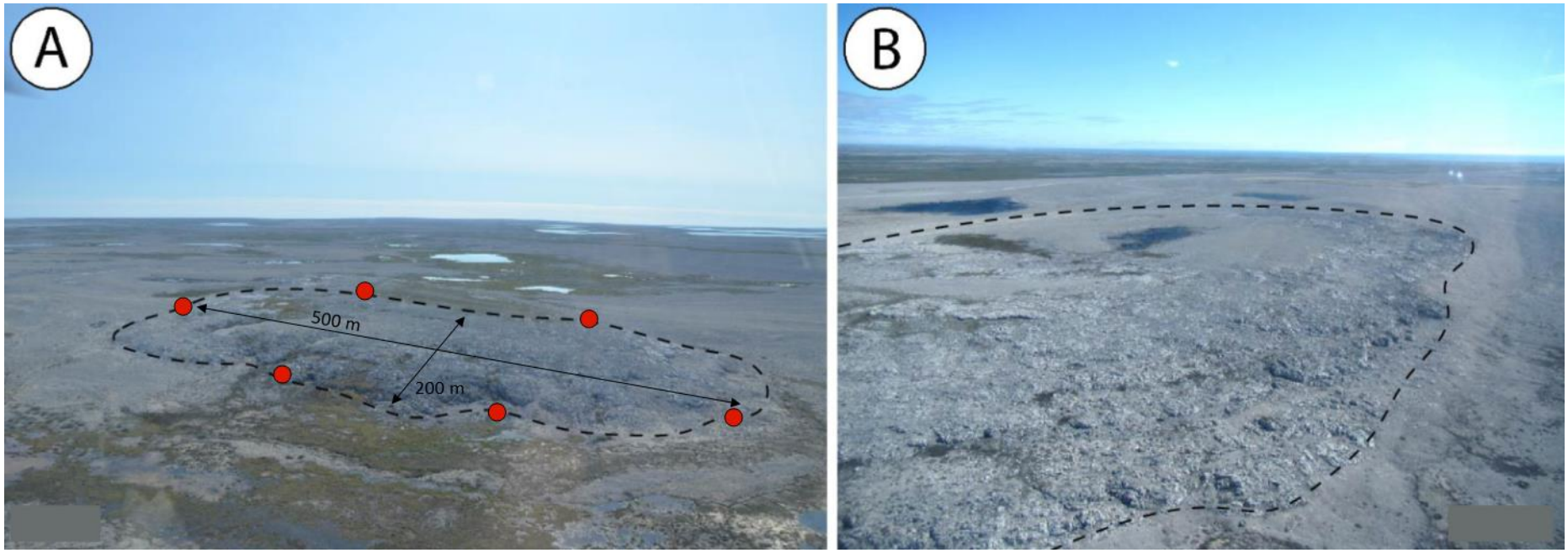

Figure 6: A – Aerial photograph of the studied RHR Fm. reefal mound looking towards the SE. Dashed line shows the outline of the mound. Red circles represent approximate section locations. B – Aerial photograph of the studied RHR Fm. reefal mound looking towards the NE. Dashed line shows the outline of the mound.

Figure 7: Field photographs showing the macroscopic facies (massive (95%, M) and stratiform (5%, S) of the RHR Formation reefal mound on Southampton Island (see text)).

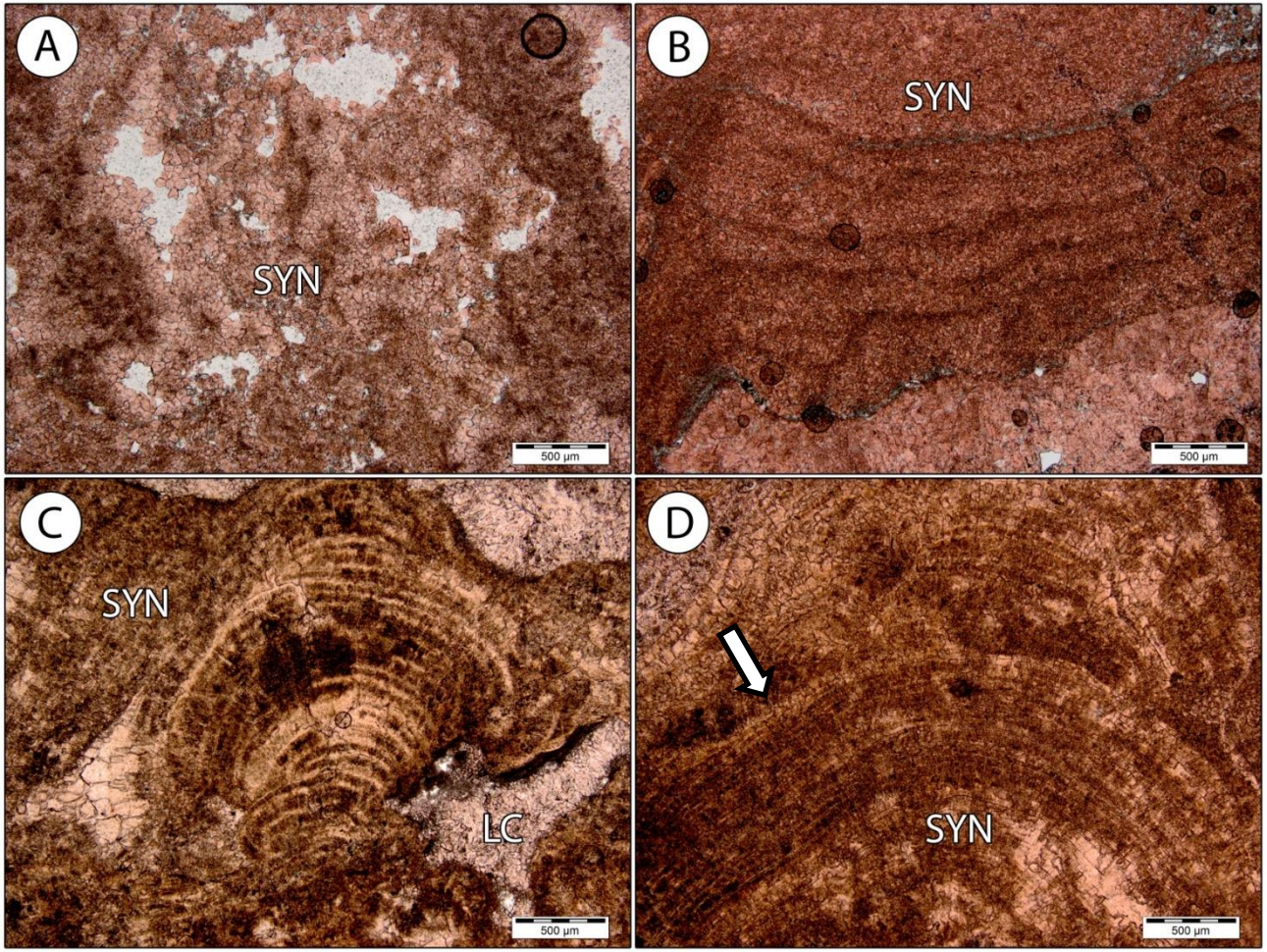

Figure 8: Photomicrographs of the synsedimentary cement component in the RHR Fm. reefal mound. A – Synsedimentary cement (SYN) showing neomorphic fabric with uneven edges and vug dissolution. B – Inclusion rich synsedimentary cement (SYN) showing cement crust fabric resulting from periodic cement precipitation. C – Botryoidal synsedimentary cement (SYN) and late cement infilling vug dissolution (LC). D – Botryoidal synsedimentary cement (SYN) showing square crystal terminations (arrow).

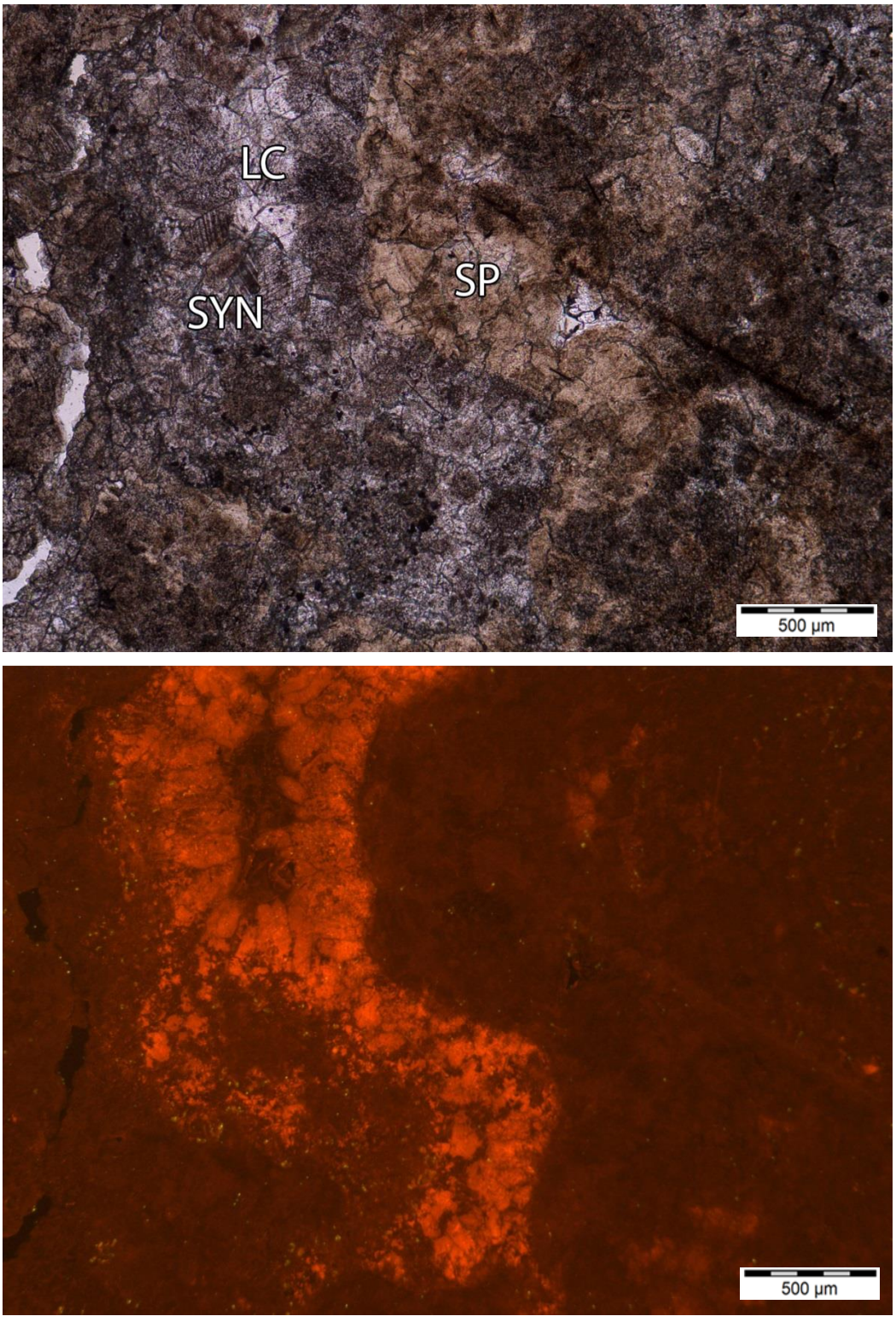

Figure 9: Paired transmitted light and CL photomicrographs of the RHR Formation showing the synsedimentary cement (SYN) with a bright orange luminescence, late cement (LC) with a non-luminescent response, and spongial tissue (SP) with a non-luminescent response. Thin section 15-65B.

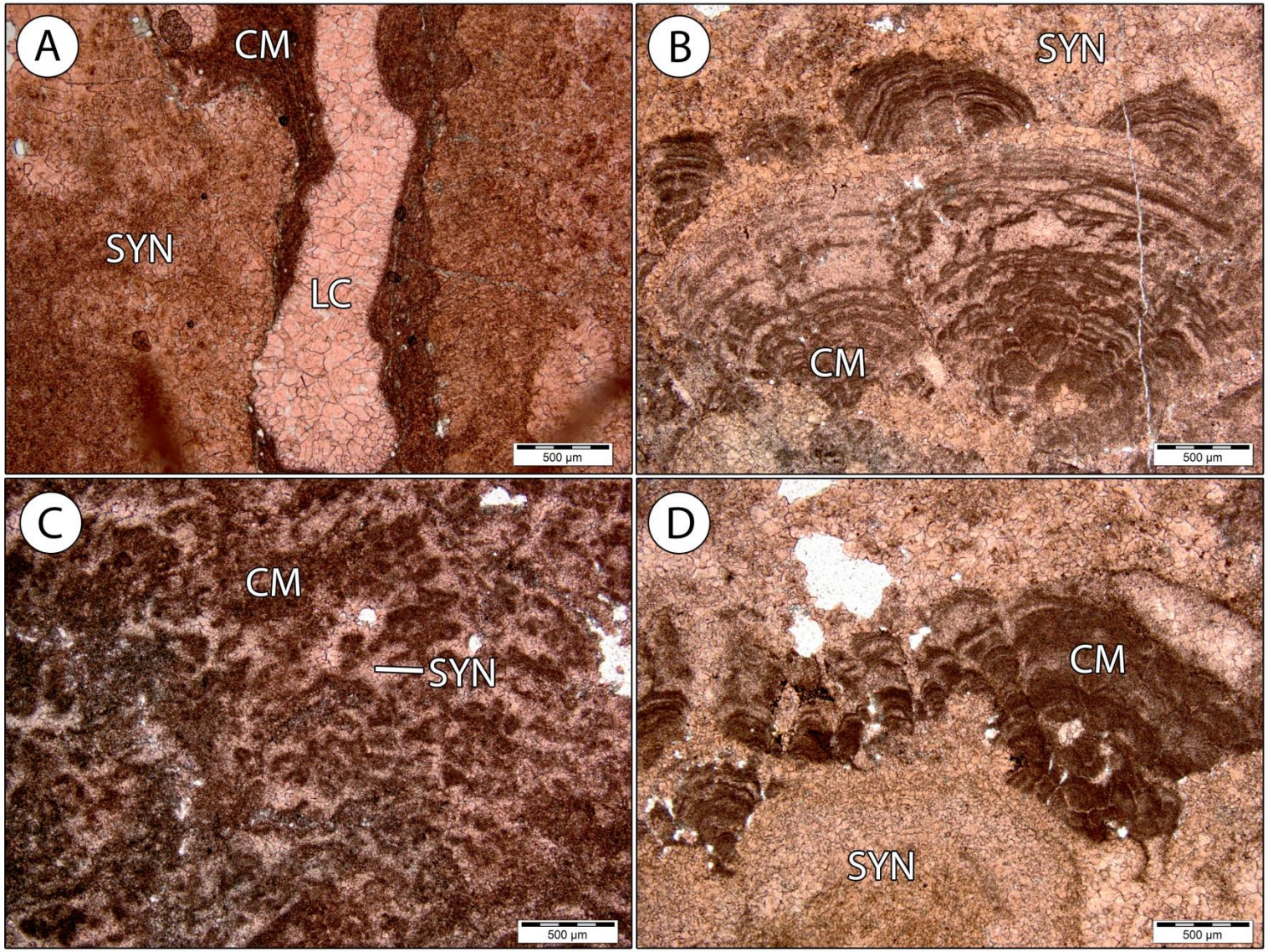

Figure 10: Photomicrographs of the calcimicrobial component in the RHR Fm. reefal mound. A – Neomorphosed coral (LC) encrusted with laminated automicrite resulting from microbial activity (CM) within synsedimentary cement (SYN). B – Calcimicrobes (CM) growing within synsedimentary cement (SYN). C – Clotted and bush-like calcimicrobes (CM) within synsedimentary cement (SYN). D – Calcimicrobes growing within synsedimentary cement (SYN).

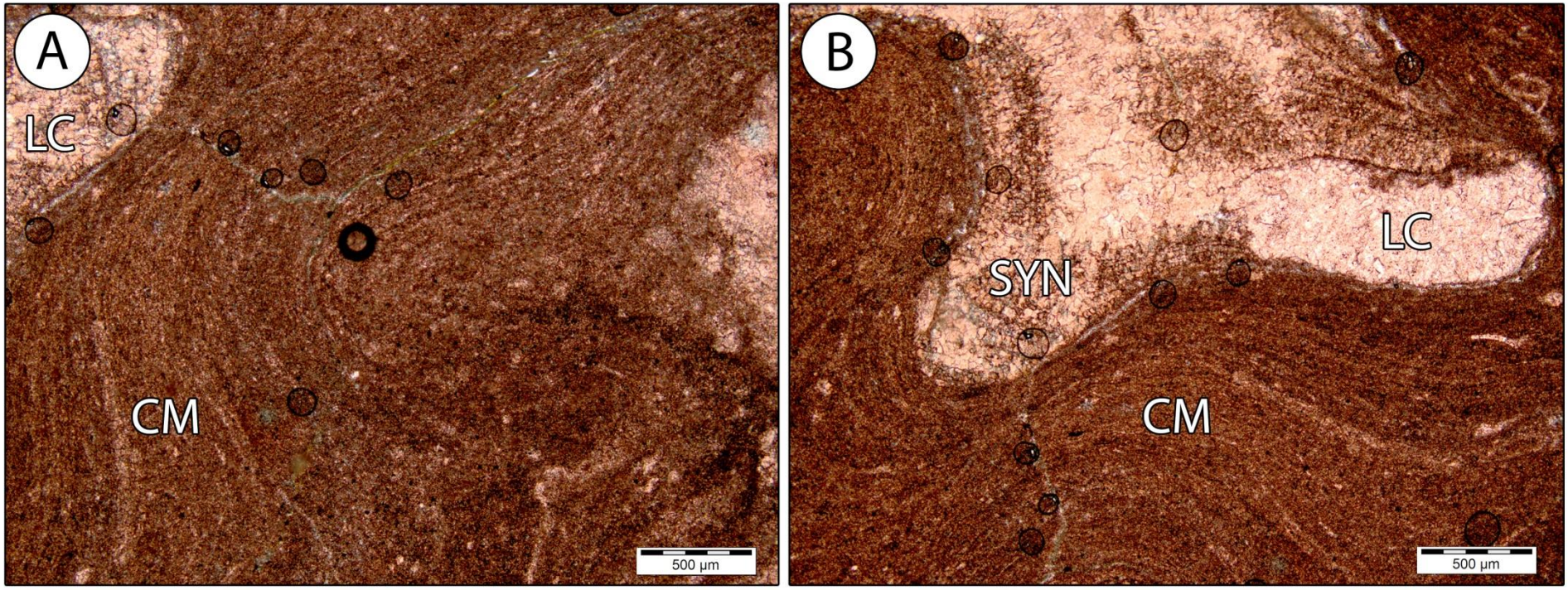

Figure 11: Photomicrographs of the laminated automicrite in the RHR Fm. reefal mound. A – Laminated automicrite resulting from microbial activity (CM) near late cement (LC). B – Laminated automicrite resulting from microbial activity (CM) near late and synsedimentary cement.

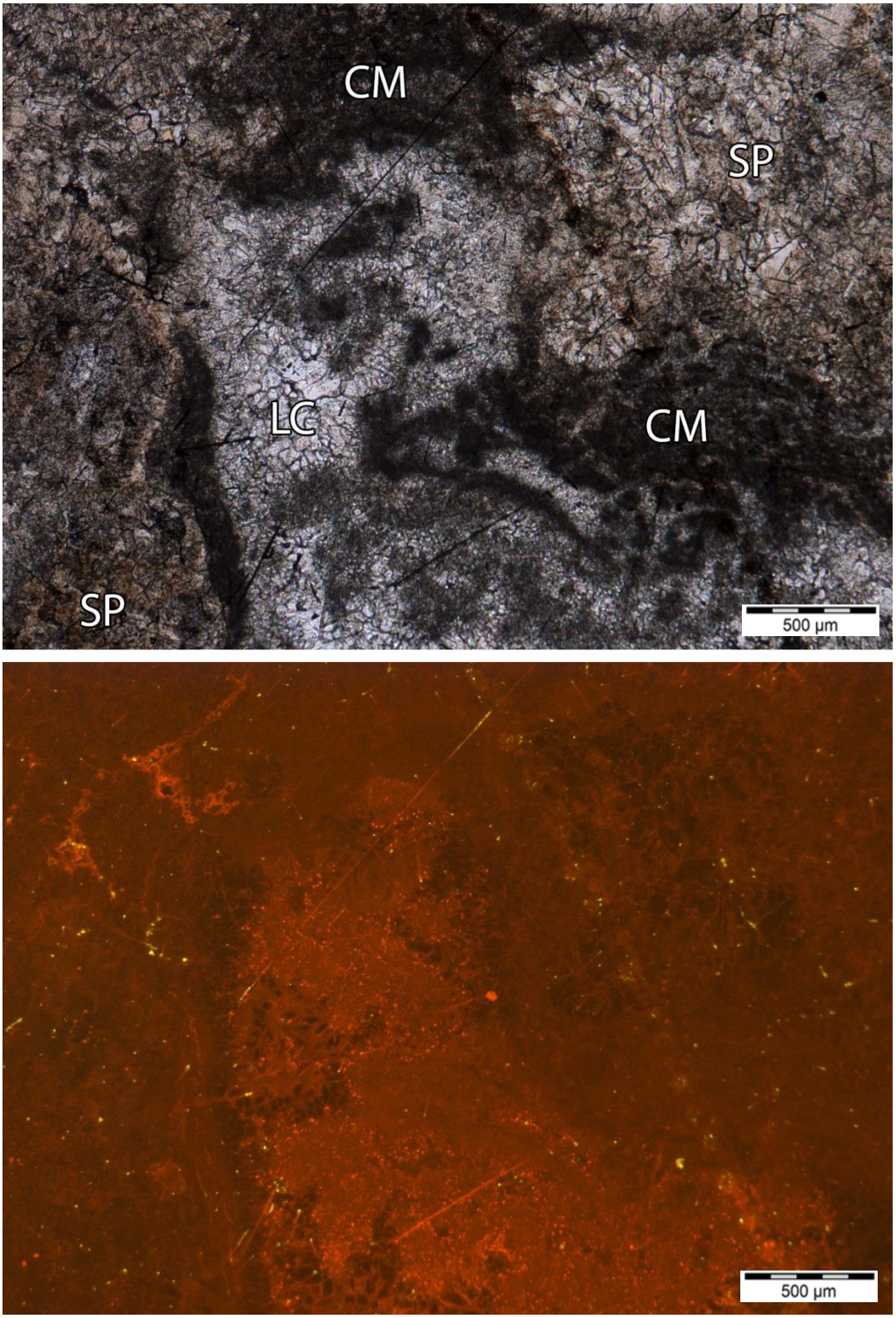

Figure 12: Paired transmitted light and CL photomicrographs of the RHR Formation showing the calcimicrobial component (CM) and spongial tissue (SP), both showing a non-luminescent response. Thin section 15-71.

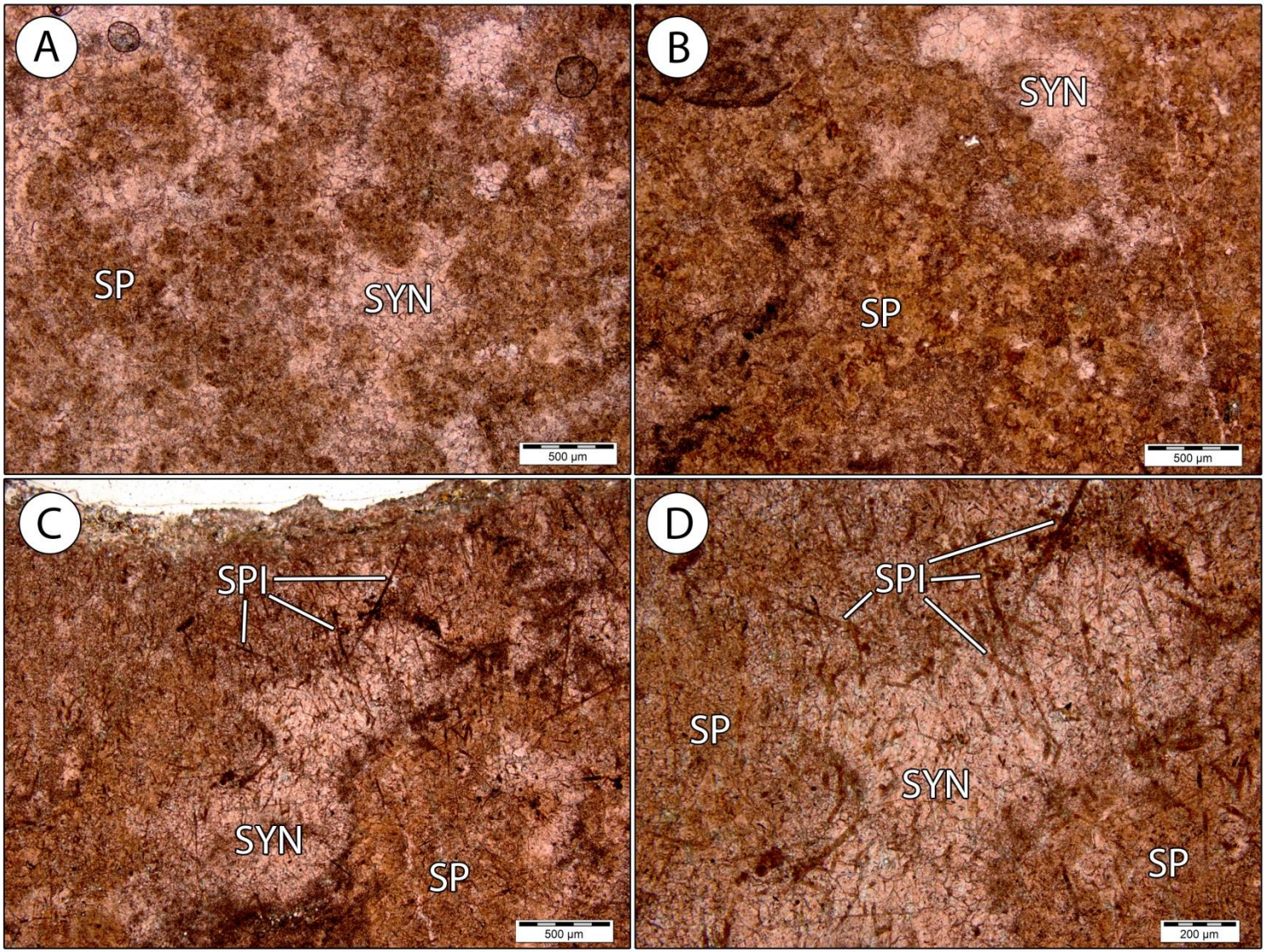

Figure 13: Photomicrographs of the sponge component in the RHR Fm. reefal mound. A – Sponge tissue (SP) showing darker yellow calcite infilled with synsedimentary cement (SYN). B - Sponge tissue (SP) showing darker yellow calcite infilled with synsedimentary cement (SYN). C - Sponge tissue (SP) showing darker yellow calcite infilled with synsedimentary cement (SYN) and showing a spicular network (SPI). D - Sponge tissue (SP) showing darker yellow calcite infilled with synsedimentary cement (SYN) and showing a spicular network (SPI)

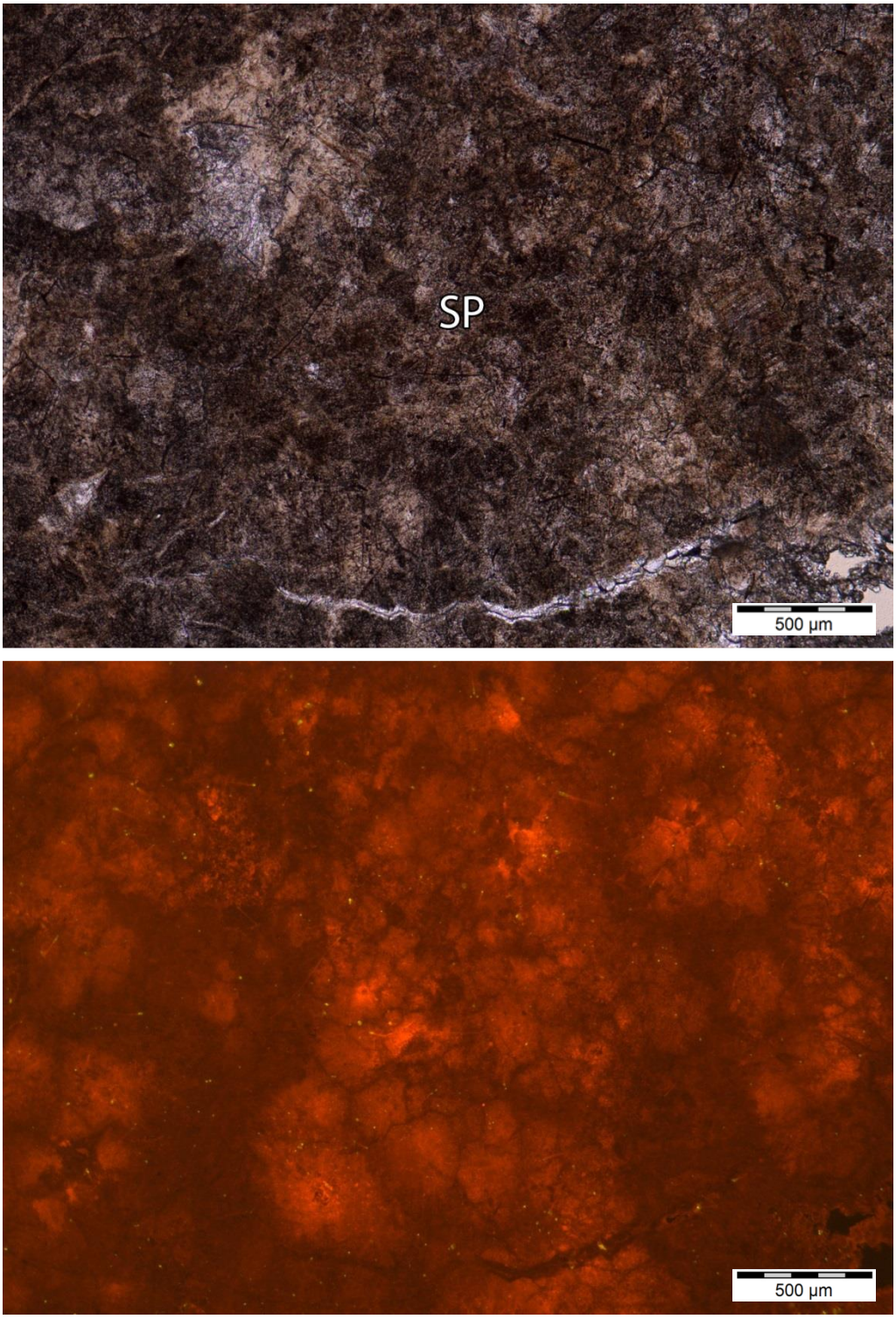

Figure 14: Paired transmitted light and CL photomicrographs of the RHR Formation showing spongial tissue (SP) with a non-luminescent to dull luminescent response and a blotchy pattern. Thin section 15-65B.

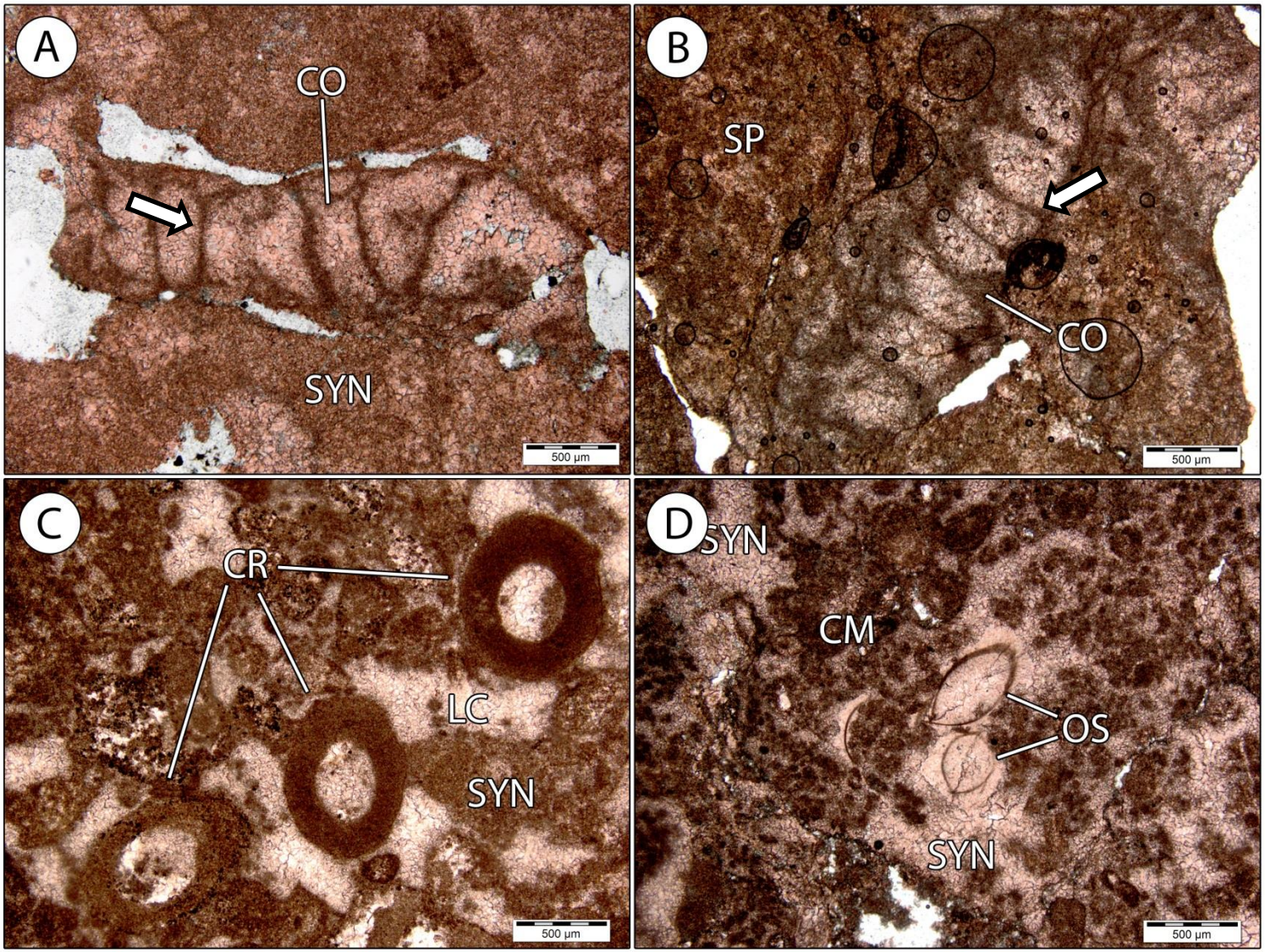

Figure 15: Photomicrographs of the metazoan component in the RHR Fm. reefal mound. A – Neomorphosed coral (CO) showing relics of septa (arrow) within synsedimentary cement (SYN). B - Neomorphosed coral (CO) showing relics of septa (arrow) within synsedimentary cement (SYN). C – Crinoids (CR) within late cement (LC) and synsedimentary cement (SYN). D – Ostracods (OS) with syntaxial overgrowth near clotted and bush-like calcimicrobes (CM) and synsedimentary cement (SYN).

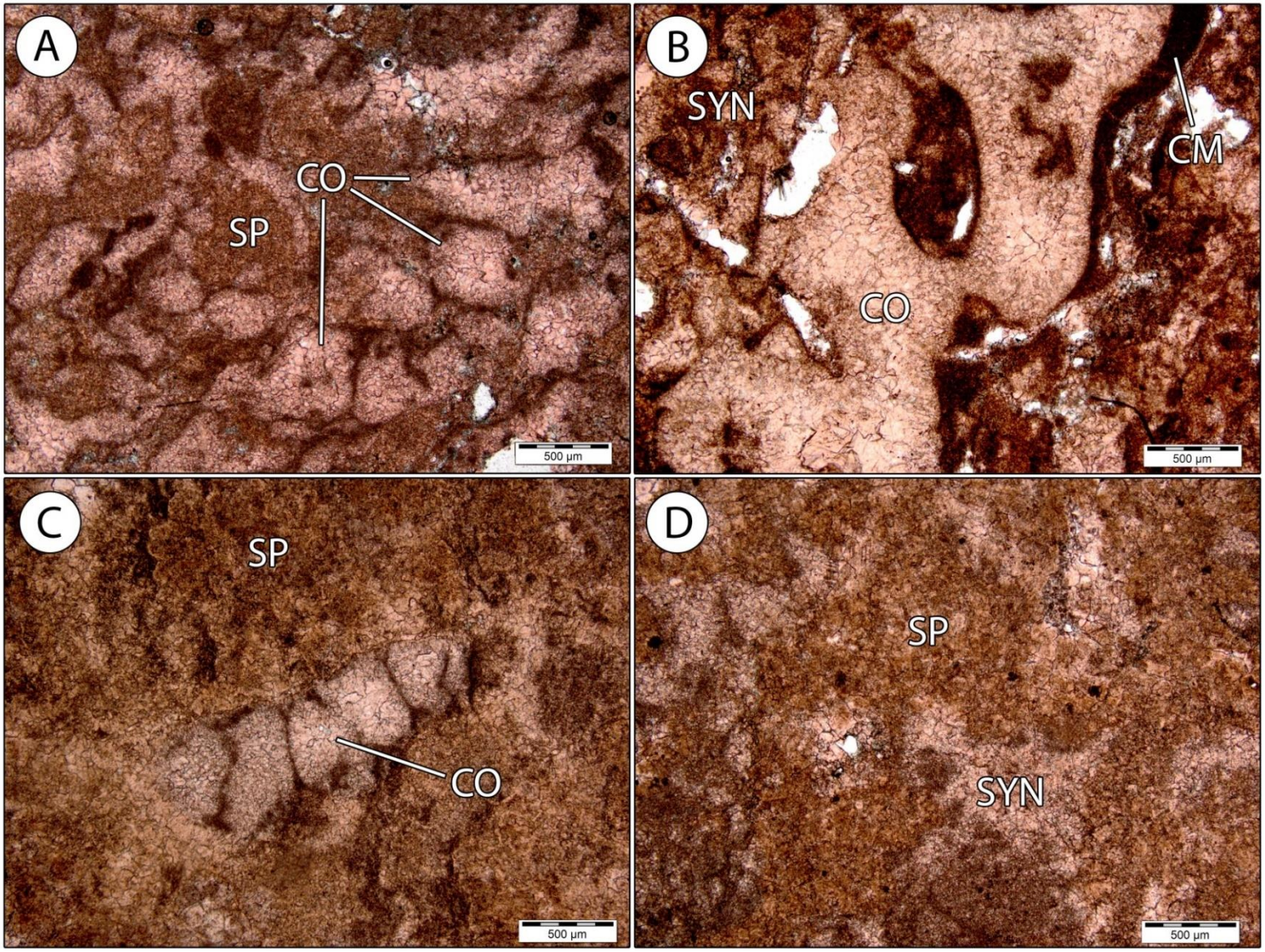

Figure 16: Photomicrographs of the boundstone facies in the RHR Fm. reefal mound. A – Coral-dominated (CO) boundstone with sponges (SP). B – Coral-dominated (CO) boundstone with calcimicrobial encrustation (CM) and synsedimentary cement (SYN). C – Sponge-dominated (SP) boundstone with minor coral (CO). D – Sponge-dominated (SP) boundstone with synsedimentary cement (SYN)

.

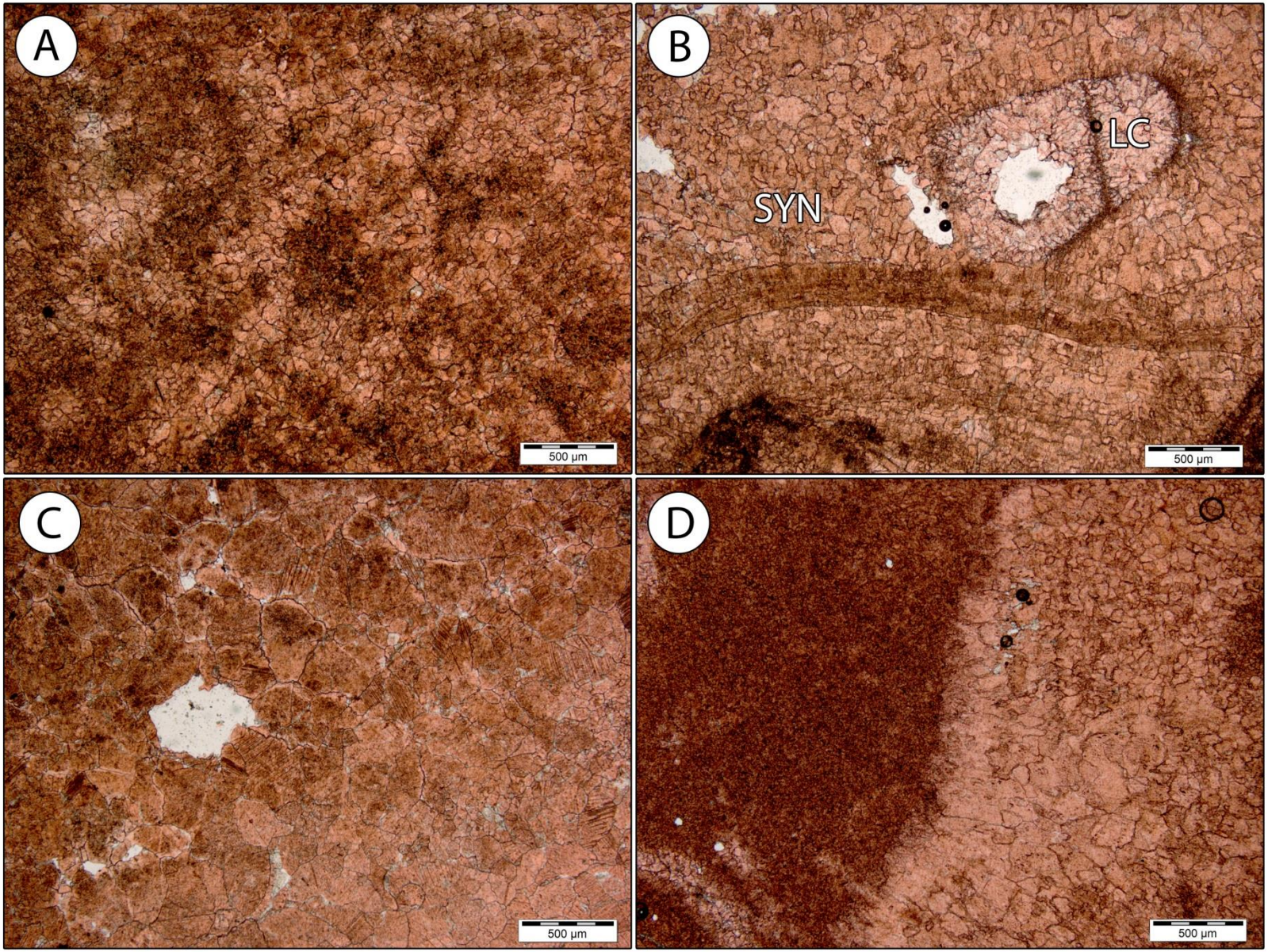

Figure 17: Photomicrographs of the cementstone facies in the RHR Fm. reefal mound. A – Granular and fibrous synsedimentary cement. B – Isopachous and granular synsedimentary cement (SYN) with square terminations with late cement (LC) infilling vug dissolution. C – Granular synsedimentary cement. D – Granular and fibrous synsedimentary cement

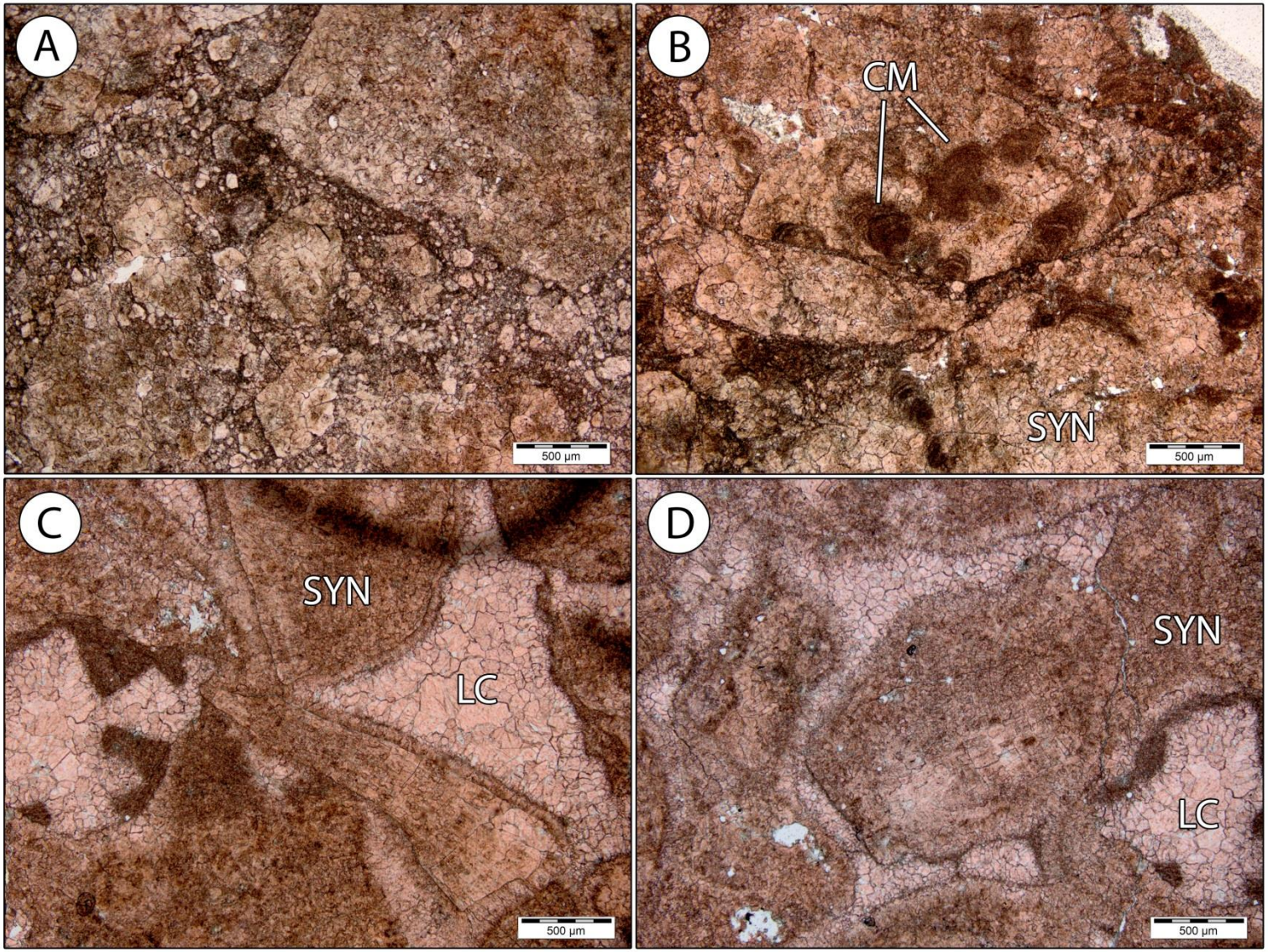

Figure 18: Photomicrographs of the rudstone facies in the RHR Fm. reefal mound. A – Angular to sub-angular inclusion-rich cement clasts. B – Angular synsedimentary cement clasts (SYN) showing calcimicrobial growth (CM). C – Angular synsedimentary cement clasts (SYN) bound by a second generation of isopachous synsedimentary cement within a late cement (LC). D – Angular to sub-angular synsedimentary cement clasts (SYN) within a late cement (LC).

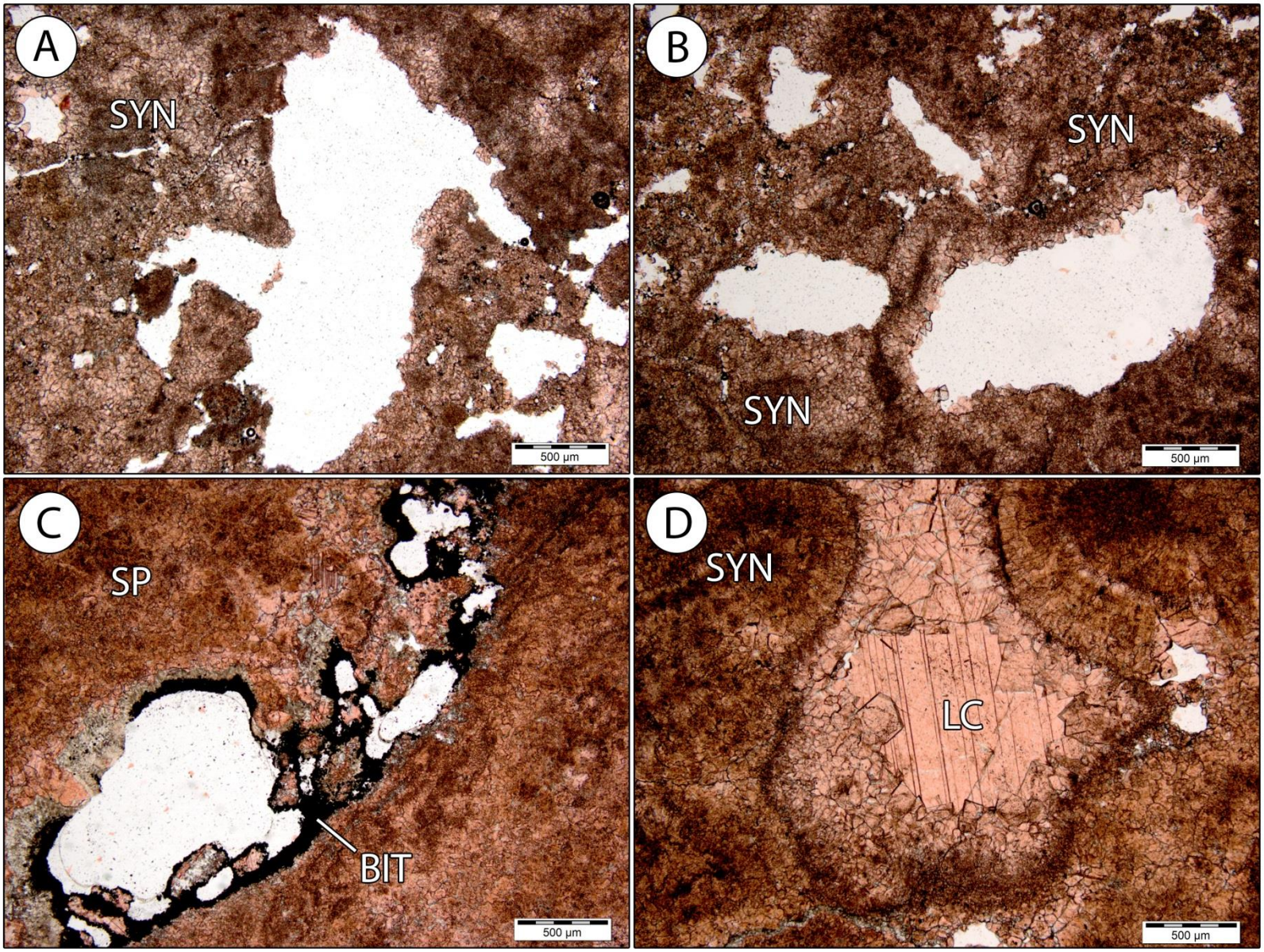

Figure 19: Photomicrographs showing dissolution vugs present in the RHR Fm. reefal A – Vugs within synsedimentary cement (SYN) cross-cutting cement fabrics. B – Vugs within synsedimentary cement. C – Bitumen (BIT) lining vug porosity near spongial tissue (SP). D – Vug filled with drusy late cement within synsedimentary cement (SYN).

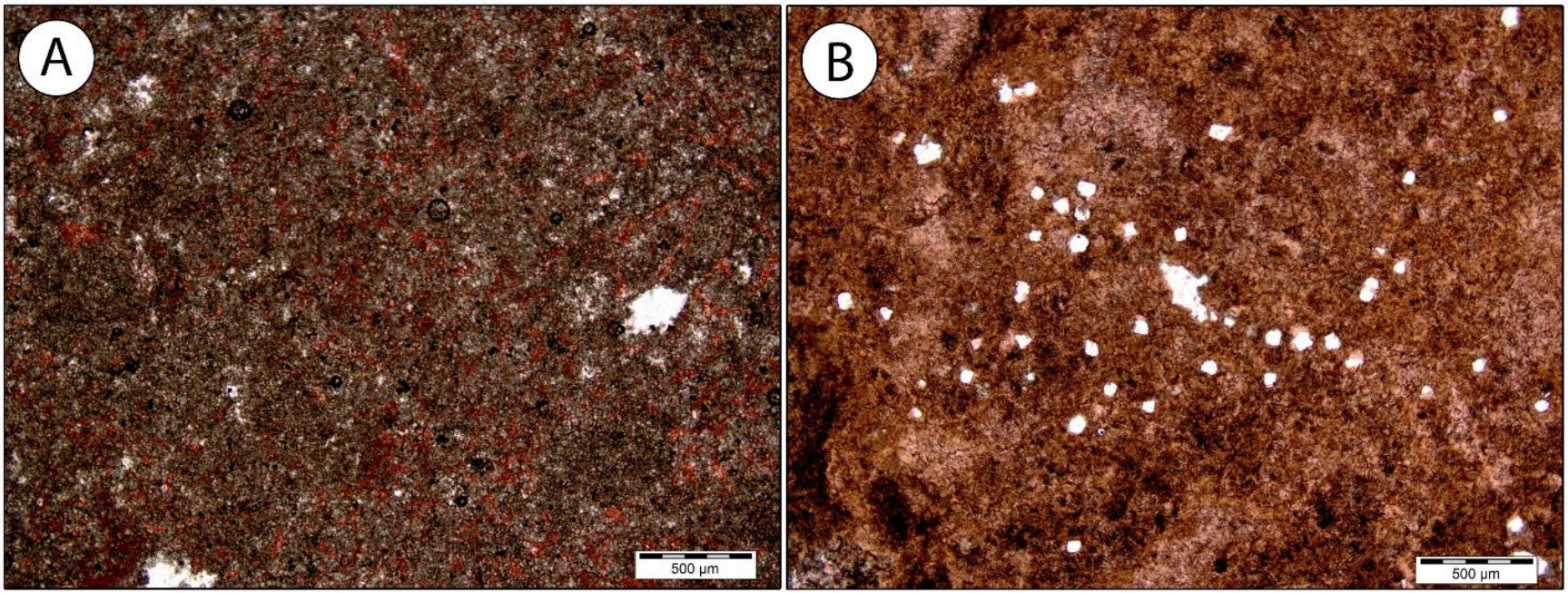

Figure 20: Photomicrographs illustrating dolomite and dedolomite phases locally present in the RHR Fm. reefal mound. A – Dolostone found within the field stratiform facies. B – Rhombohedral pores resulting from dedolomitization processes.

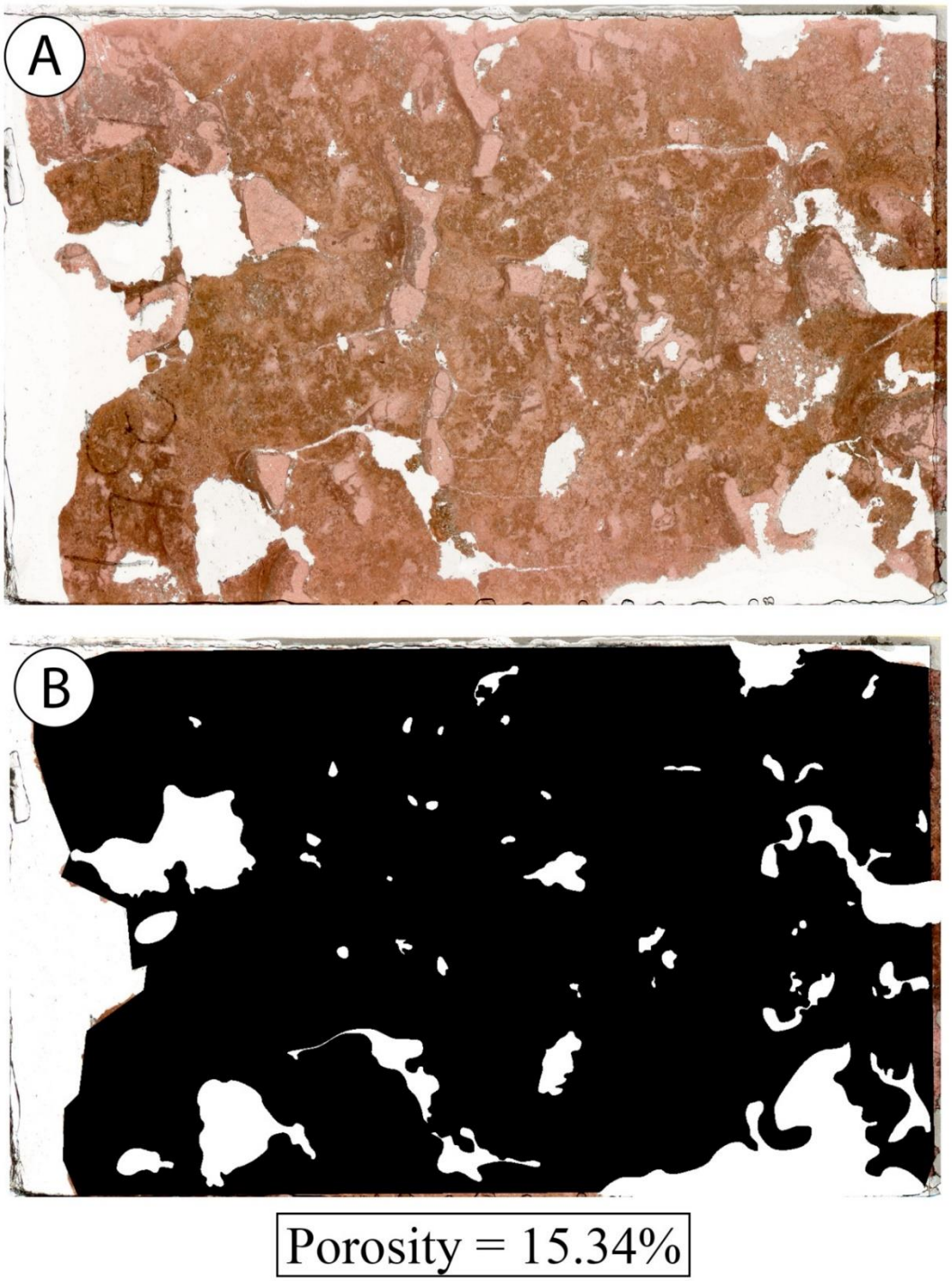

Figure 21: A – Scan of thin section 15-34 (3x5 cm). B - Digital mapping of thin section 15-34 from section #2 showing porosity (white) and non-porosity (black). The porosity in this thin section was calculated to be approximately 15.34%.

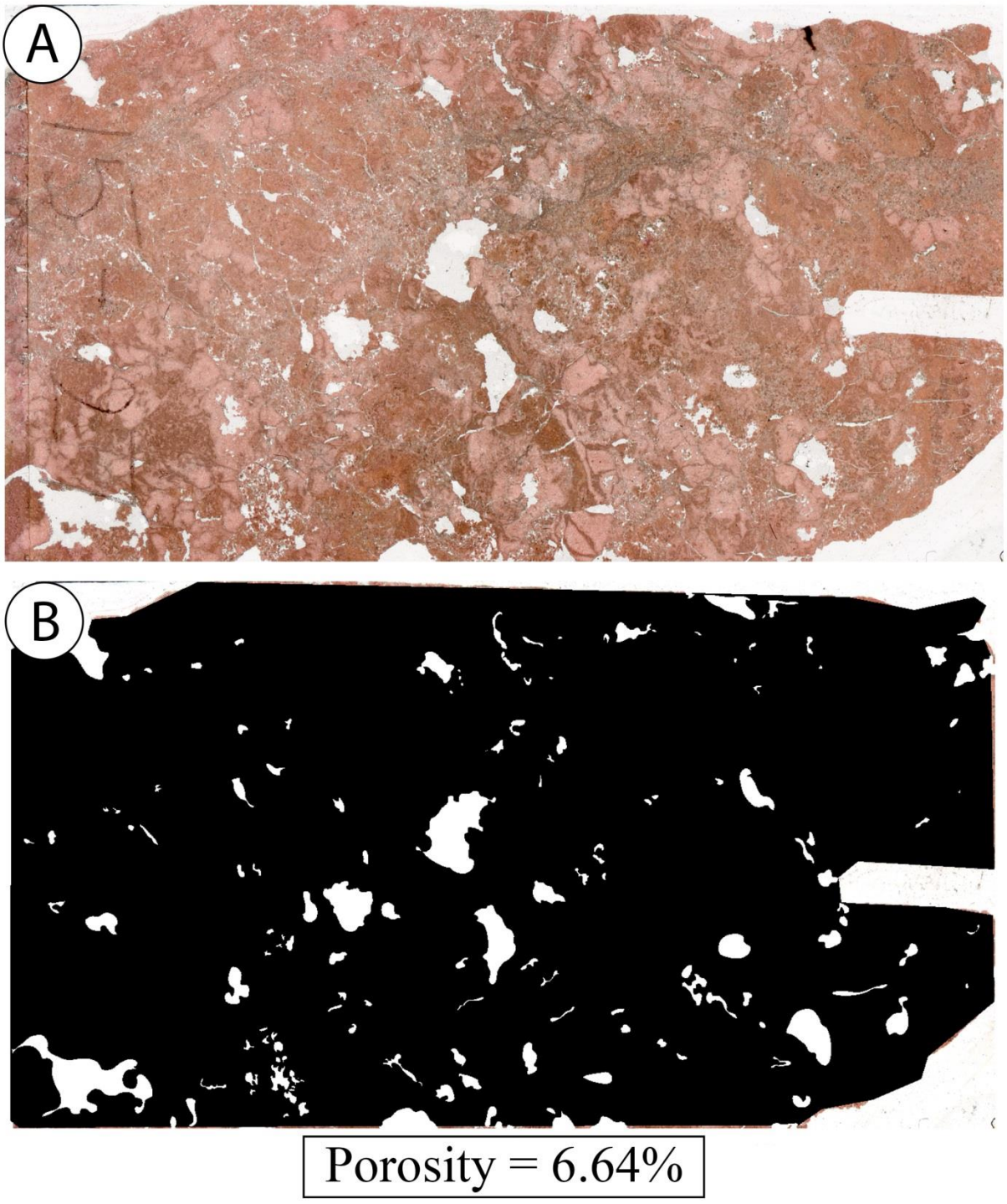

Figure 22: A – Scan of thin section 15-27 (3x5 cm). B - Digital mapping of thin section 15-27 from section #3 showing porosity (white) and non-porosity (black). The porosity in this thin section was calculated to be approximately 6.64%.

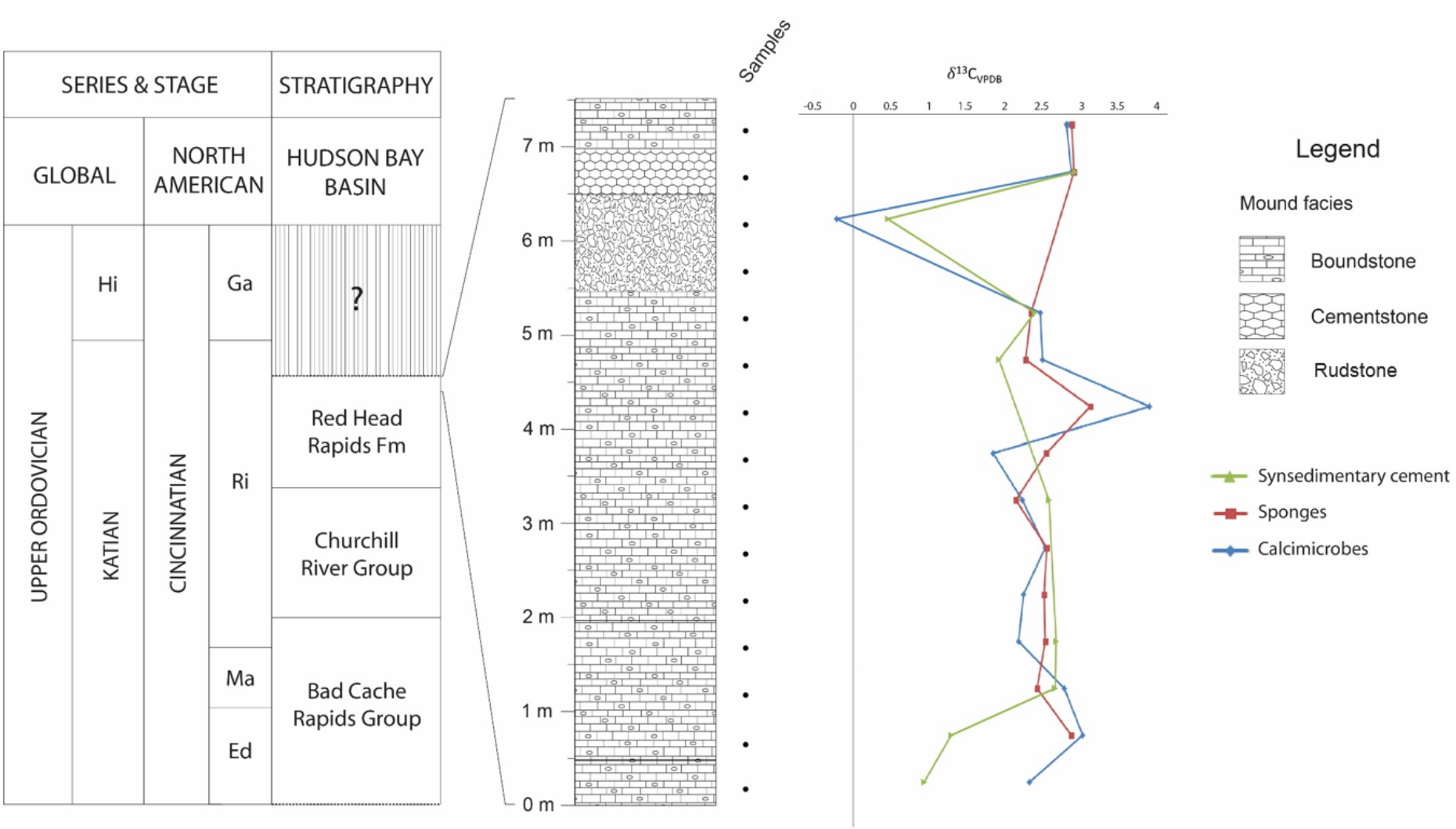

Figure 23: Chemostratigraphic $\delta^{13}C$ curve for section #6 of the mound.

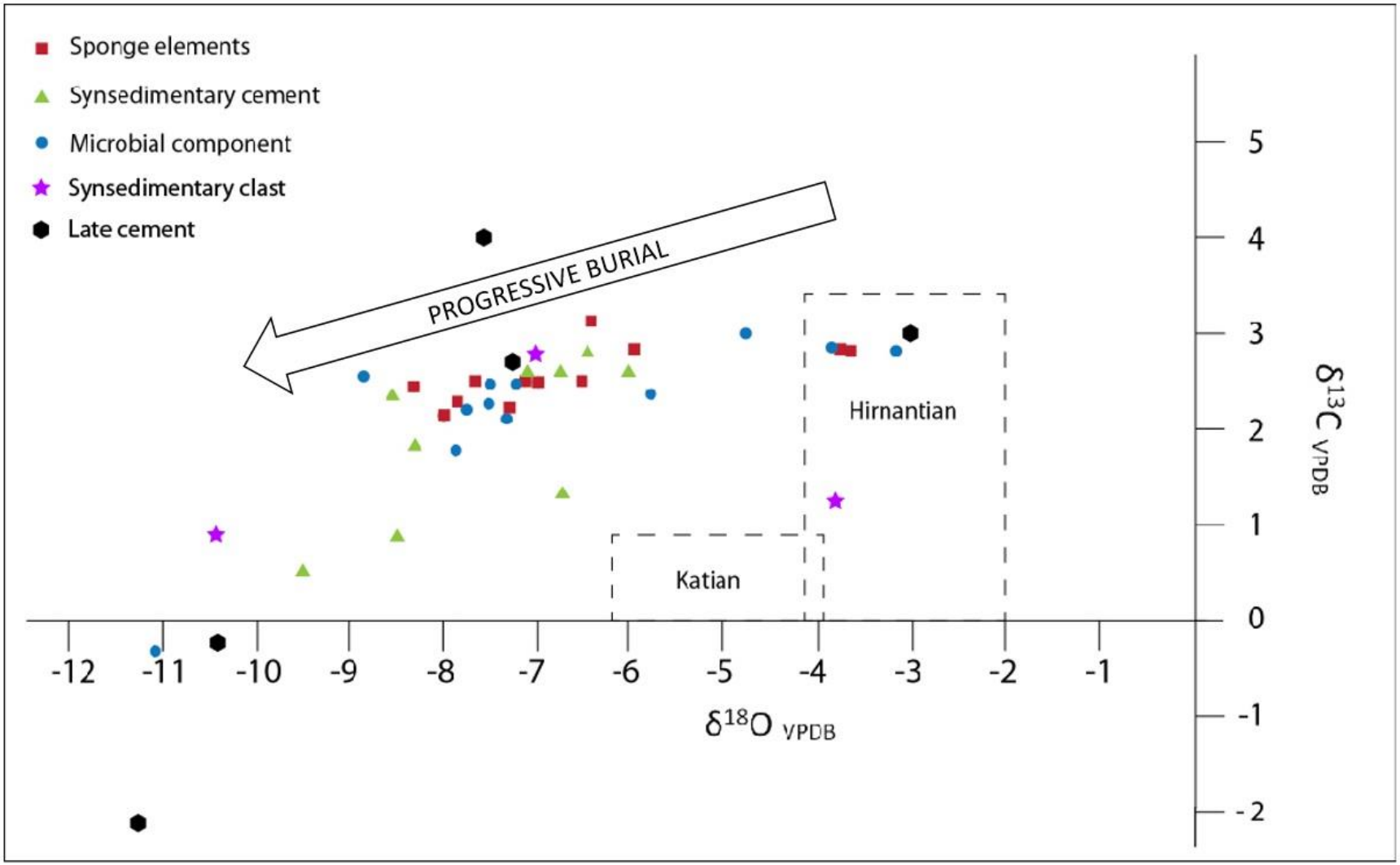

Figure 24: Cross plot of $\delta^{13}C$ versus $\delta^{18}O$ for various components present in the RHR Fm. reefal mound. Dashed boxes show variations in typical seawater values of $\delta^{13}C$ and $\delta^{18}O$ for the Katian and the Hirnantian based on brachiopods (Shields et al. 2003). Arrow shows the burial trend.

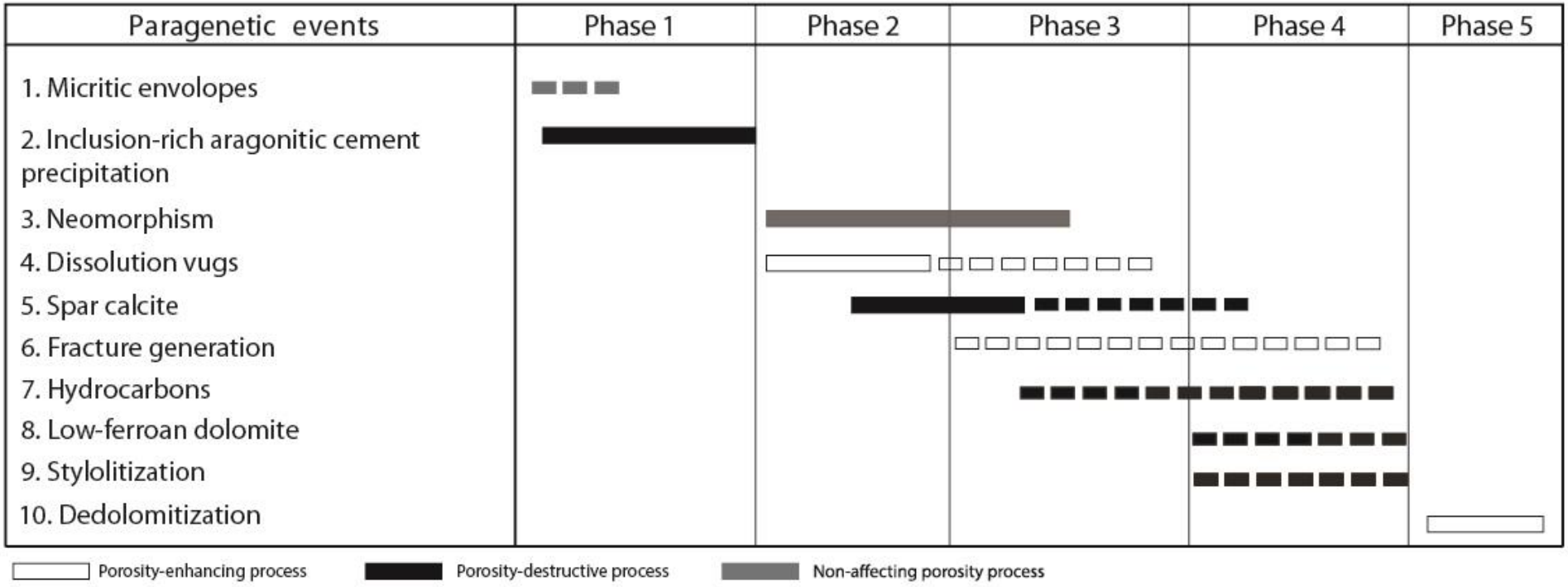

Figure 25: Paragenetic sequence of the RHR Fm. reef mound showing 10 paragenetic events and 5 phases.

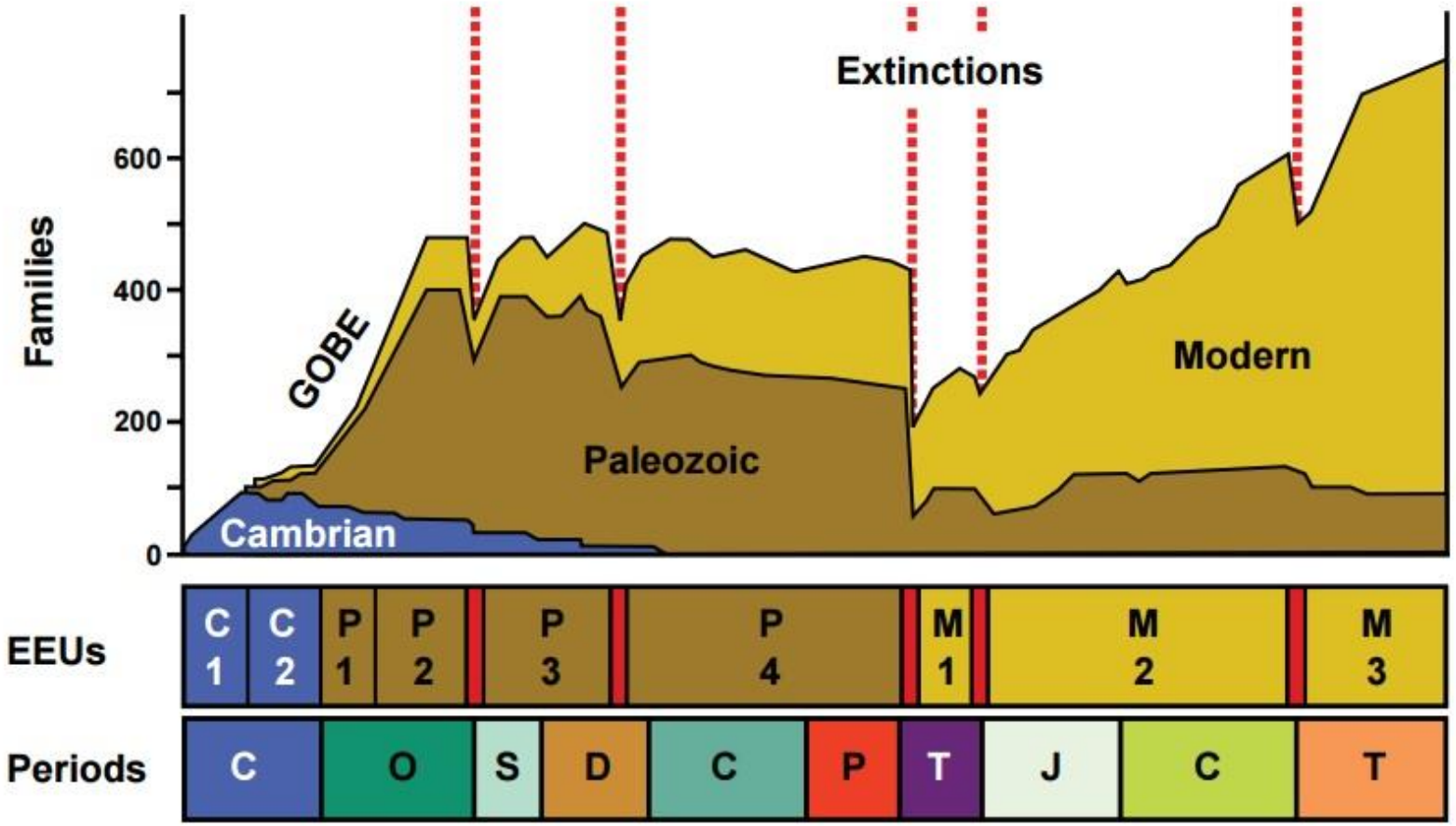

Figure 27: Diversity curve of marine invertebrate families through Phanerozoic time documenting the GOBE and the five mass extinctions of marine invertebrates. P1–4—Paleozoic; M1–3—Modern. Geological periods, from left to right: C—Cambrian; O—Ordovician; S—Silurian; D—Devonian; C—Carboniferous; P—Permian; T—Triassic; J–Jurassic; C—Cretaceous; T—Tertiary. Servais et al. 2009

Appendix

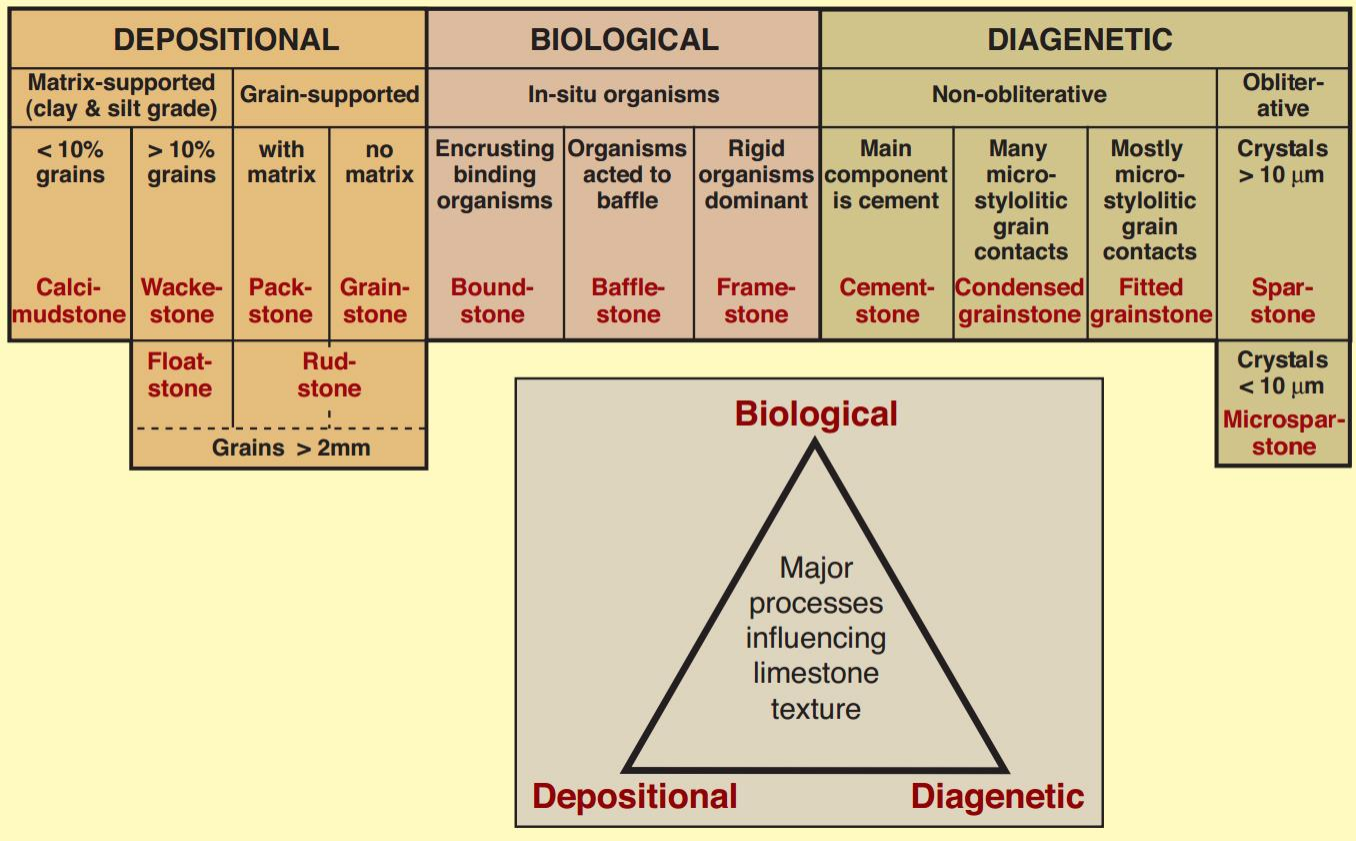

Figure 1: Wright's 1992 classification of microfacies (Scholle and Ulmer-Scholle, 2003)

	Frame						Cements		Porosity	Name
	Metazoan			Automicrite		Calcimicrobes	Primary cement	Pore-filling cement		
ID #	Coral	Sponges	Others	Peloidal	Laminated		(inclusion rich)	(drusy)		
3	30-40%	None	None	None	None	5-10%	45-55%	5%	5-10%	Coral boundstone
4	5%	None	None	None	None	5-10%	80-85%	5%	10-15%	Cementstone
5	5%	5%?	None	None	None	15-20%	65-70%	5%	5-10%	Calcimicrobial cementstone
6	5%	40-50%?	None	None	5%	10-15%	25-35%	5%	5-10%	Sponge boundstone
7	15-20%	50-60%	None	None	None	10-15%	10-15%	None	10-15%	Coral rich sponge boundstone
8	None	None	None	None	None	5-10%	80-90%	5-10%	5%	Calcimicrobial cementstone
9	None	None	None	None	5-10%	20-25%	50-60%	10-15%	5%	Calcimicrobial cementstone
10	None	None	None	None	None	None	95%	5%	10-15%	Cementstone
11	5-10%	None	None	None	None	5-10%	75-85%	5%	5-10%	Cementstone
12	None	None	Crinoids - 5-10%	None	5-10%	40-50%	30-40%	10-15%	5%	Calcimicrobial boundstone
13	None	None	None	None	None	35-40%	50%	10-15%	5%	Calcimicrobial boundstone
14	25-35%	None	Strom? 15-20%	None	None	10-15%	15-20%	5-10%	10-15%	Calcimicrobial coral boundstone
15	5%	50-60%	None	None	None	5-10%	20-30%	5%	10-15%	Calcimicrobial sponge boundstone
16	5%	40-50%	None	None	None	10-15%	25-35%	5%	10-15%	Calcimicrobial sponge boundstone
17	None	60-70%	None	None	None	5-10%	15-20%	5%	5-10%	Sponge boundstone
18	10-15%	None	None	None	None	30-40%	35-45%	5-10%	5-10%	Calcimicrobial coral boundstone
19	None	25-35%?	None	None	None	5%	40-50%	10-15%	5-10%	Sponge boundstone

Table 1: Petrographic observations for for section #1 samples.

	Frame						Cements		Porosity	Name
	Metazoan			Automicrite		Calcimicrobes	Primary cement	Pore-filling cement		
ID #	Coral	Sponges	Others	Peloidal	Laminated		(inclusion rich)	(drusy)		
20	None	None	Cephalopod and possible stromatoporoid	None	None	15-20%	40-50%	15-20%	10-15%	Calcimicrobial boundstone
21	Yes?	?	?	No	No	No	Unsure	Unsure	20%	Coral rich cement stone
22	5%	No	No	No	No	10-15%	70-80%	5%	25-30%	Calcimicrobial cementstone
23	5%	None	None	None	Yes	20-25%	50-60%	5-10%	10-15%	Cementstone
24	None	None	None	None	None	None	None	None	<5%	Dolostone
25	5%	60-70%	No	No	No	25-30%	Yes?	10%	15-20%	Calcimicrobial sponge boundstone
26	10-15%	30-40%	No	No	No	15%	30-35%	5%	5-10%	Calcimicrobial sponge boundstone
27	10-20%	30-40%	No	5-10%	No	15-20%	15-20%	5%	20%	Calcimicrobial coral boundstone
28	10-15%	10-15%	No	No	No	5-10%	50-60%	5%	30-35%	Coral-rich sponge boundstone
29	10-20%	None	No	10-15%	No	5%	50-60%	0%	10-15%	Calcimicrobial coral boundstone
30	5-10%	10-20%	No	No	No	40-50%	10-20%	5-10%	10-15%	Calcimicrobial sponge boundstone
31	5-10%	50-60%	No	No	No	15-20%	10%	5%	15-20%	Calcimicrobial sponge boundstone
32	None	None	None	No	None	30-40%	40-50%	5-10%	5-10%	Microbial cementstone
33	5-10%	No	Rugose colony	5-10%	10-20%	Unsure	No	10-20%	15-20%	Calcimicrobial rugose boundstone
34	5-10%	60-70%	Possibly gastropod	No	5-10%	10-20%	Maybe 5%	5-10%	20-30%	Calcimicrobial coral-rich sponge boundstone
35	No	None	No	In clasts	5%	0%	In clasts	15-20%	10-15%	Rudstone

Table 2: Petrographic observations for section #2 samples.

	Frame						Cements		Porosity	Name
	Metazoan			Automicrite		Calcimicrobes	Primary cement	Pore-filling cement		
ID #	Coral	Sponges	Others	Peloidal	Laminated		(inclusion rich)	(drusy)		
36	10-20%	None	None	20-30%	None	None	40-50%	5%	15-20%	Coral boundstone
37	Less than 5%	15%	Possibly?	None	None	35%	50%	5-10%	15-20%	Calcimicrobial cementstone
38	Less than 5%	10-15%	None	None	None	25-30%	50-60%	None	5-10%	Calcimicrobial cementstone
39	5-10%	50%	None	None	None	20%	20%	5%	5-10%	Calcimicrobial sponge boundstone
40	Less than 5%	50-60%	Possibly?	None	None	30%	10-20%	5%	5-10%	Calcimicrobial sponge boundstone
41	5%	30-40%	None	None	Less than 5%	10-20%	30-40%	5%	10-15%	Cement-rich sponge boundstone
42	10-20%	None	None	None	None	30-40%	40-50%	None	5-10%	Calcimicrobial coral boundstone
43	5-10%	None	Yes - crinoids and ostracods	5-10%	None	20%	30%	5%	5%	Crinoid rich calcimicrobial boundstone
44	25-30%	None	None	None	None	10-20%	30-40%	5%	10-15%	Calcimicrobial coral boundstone
46	10-20%	None	None	None	None	10-15%	50-60%	None	10-15%	Calcimicrobial coral boundstone
47	5%	None	None	None	None	None	90-95%	None	10-20%	Cementstone
48	None	None	None	None	None	None	90-100%	5%	5-10%	Cementstone
49	None	None	None	None	None	40-50%	40-50%	5%	10-15%	Calcimicrobial cementstone
50	None	None	None	None	None	40-50%	50-60%	5%	10-15%	Calcimicrobial cementstone

Table 3: Petrographic observations for section #3 samples.

	Frame						Cements		Porosity	Name
	Metazoan			Automicrite		Calcimicrobes	Primary cement	Pore-filling cement		
ID #	Coral	Sponges	Others	Peloidal	Laminated		(inclusion rich)	(drusy)		
51	15-25%	15-25%	None	None	5-10%	5%	30%	None	10-15%	Coral rich sponge boundstone
52	5%	None	None	Less than 5%	Less than 5%	None	80%	None	10-15%	Breccia
53	10-15%	None	None	None	None	20-30%	60-70%	5%	10-15%	Coral rich calcimicrobial boundstone
54	15-20%	None	None	None	20-30%	5-15%	40-50%	None	15%	Coral rich calcimicrobial boundstone
55	15-25%	5-10%	None	None	None	30-35%	30-40%	None	15-20%	Coral rich calcimicrobial boundstone

Table 4: Petrographic observations for section #4 samples.

	Frame						Cements		Porosity	Name
	Metazoan			Automicrite		Calcimicrobes	Primary cement	Pore-filling cement		
ID #	Coral	Sponges	Others	Peloidal	Laminated		(inclusion rich)	(drusy)		
56	None	None	None	None	None	60-70%	10-20%	5-10%	10-20%	Calcimicrobial cementstone
57	None	None	10-20%	None	None	50-60%	20-30%	5-10%	30-40%	Crinoid rich calcimicrobial boundstone
58	None	None	None	None	None	None	100%	None	20-30%	Cementstone
58A	None	None	None	None	None	None	100%	None	10-20%	Cementstone
59	10-15%	None	None	None	None	5-10%	60-70%	5%	10-15%	Cementstone
61	20-30%	None	None	None	None	5-10%	50-60%	< 5%	10-20%	Cementstone to coral boundstone
62	5%	None	None	None	None	10-20%	60-70%	5%	10%	Calcimicrobial cementstone
63	None	None	None	None	None	5-10%	80%	5-10%	5%	Cementstone
64	None	None	15-25%	None	None	30-40%	30-40%	5-10%	15-25%	Crinoid rich calcimicrobial boundstone
65	5-10%	None	None	None	None	5-10%	75-85%	5-10%	5%	Cementstone
66	5-10%	None	None	None	None	5-10%	70-80%	10-15%	5-10%	Cementstone
67	None	5-10%?	None	None	None	10-15%	7-80%	5%	5%	Cementstone
68	10-20%	None	None	None	None	10-20%	60-70%	5-10%	5-10%	Calcimicrobial coral boundstone
69	None	20-30%	None	None	None	30-40%	15-25%	15-20%	10-15%	Calcimicrobial sponge boundstone
70	None	None	None	None	None	10-20%	70-80%	5-10%	5-10%	Calcimicrobial cementstone
71	None	30-40%	None	None	None	10-20%	30-40%	10-15%	10-20%	Calcimicrobial sponge boundstone
72	20-30%	20-30%	None	None	Yes	15-25%	10-20%	5%	20-25%	Coral rich sponge boundstone

Table 5: Petrographic observations for section #5 samples.

	Frame						Cements		Porosity	Name
	Metazoan			Automicrite		Calcimicrobes	Primary cement	Pore-filling cement		
ID #	Coral	Sponges	Others	Peloidal	Laminated		(inclusion rich)	(drusy)		
73	None	None	None	None	None	60-70%	15-20%	10-15%	10-15%	Calcimicrobial boundstone?
74	5%	60-70%	None	None	Yes	10-15%	5-10%	5-10%	5-10%	Calcimicrobial sponge boundstone
75	None	30-40%	None	None	None	10-15%	20-30%	5-10%	10-20%	Calcimicrobial sponge boundstone
76	5%	40-50%	None	None	Yes	10-15%	25-35%	10-15%	10-15%	Calcimicrobial sponge boundstone
77	5%	40-50%	None	None	None	5-10%	20-30%	5-10%	10-15%	Coral rich sponge boundstone
78	5-10%	40-50%	None	None	None	10-15%	20-30%	5-10%	15-20%	Coral rich sponge boundstone
79	5-10%	50-60%	None	None	None	5-10%	10-20%	5%	10-15%	Coral rich sponge boundstone
80	5-10%	50-60%	None	None	None	5-10%	10-20%	5-10%	5-10%	Coral rich sponge boundstone
81	5%	50-60%	None	None	Yes	15-20%	5-10%	5-10%	5-10%	Coral rich sponge boundstone
82	5%	40-50%	None	None	Yes	10-15%	15-20%	5-10%	5-10%	Coral rich sponge boundstone
83	5-10%	50-60%	None	None	Yes	5-10%	15-20%	5%	10-15%	Coral rich sponge boundstone
84	None	None	None	None	None	None	100%	None	less than 5%	Breccia
85	None	None	None	None	Yes	40-50%	5-10%	0%	less than 5%	Breccia? Intraclasts.
86	5%	5-10%	None	None	None	20-30%	50-60%	5-10%	10-15%	Calcimicrobial cementstone
87	5-10%	30-40%	None	None	None	20-30%	20-30%	5%	10-15%	Calcimicrobial sponge boundstone

Table 6: Petrographic observations for section #6 samples.

Sample	Component	Delta 13C (‰)	Delta 18O (‰)
73-1	Calcimicrobes	2.32	-5.78
73-2	Late cement	-2.14	-11.31
73-3	Synsedimentary cement	0.93	-8.55
74-1	Sponge	2.87	-3.63
74-2	Calcimicrobes	3.02	-4.77
74-3	Synsedimentary cement	1.29	-6.74
75-1	Calcimicrobes	2.78	-6.79
75-2	Synsedimentary cement	2.66	-7.13
75-3	Sponge	2.42	-8.34
76-1	Calcimicrobes	2.18	-7.36
76-2	Sponge	2.53	-6.5
76-3	Synsedimentary cement	2.67	-5.99
77-1	Sponge	2.51	-7.18
77-2	Calcimicrobes	2.24	-7.74
77-3	Late cement	-0.15	-10.41
78-1	Calcimicrobes	2.53	-7.23
78-2	Sponge	2.55	-6.98
79-1	Calcimicrobes	2.23	-7.46
79-2	Sponge	2.14	-7.98
79-3	Synsedimentary cement	2.58	-6.78
80-1	Calcimicrobes	1.84	-7.9
80-2	Sponge	2.54	-7.58
81-1	Calcimicrobes	3.9	-5.75
81-2	Sponge	3.12	-6.4
82-1	Calcimicrobes	2.49	-8.85
82-2	Sponge	2.27	-7.37
82-3	Synsedimentary cement	1.92	-8.35
83-1	Calcimicrobes	2.46	-7.54
83-2	Sponge	2.34	-7.88
83-3	Synsedimentary cement	2.39	-8.51
84-1	Clast	1.04	-9.04
84-2	Clast	2.87	-7.05
85-1	Clast	0.94	-10.5
85-2	Synsedimentary cement	0.45	-9.51
85-3	Calcimicrobes	-0.22	-11.06
86-1	Calcimicrobes	2.87	-6.84
86-2	Sponge	2.91	-5.94
86-3	Late cement	2.8	-7.14
86-4	Synsedimentary cement	2.92	-6.46
87-1	Calcimicrobes	2.81	-3.81
87-2	Sponge	2.88	-3.72
87-3	Calcimicrobes	2.83	-3.19
87-4	Late cement	3	-2.99
87-5	Late cement	-1.43	-12.34

Table 7: Results of isotopic analyses for section #6.

An unusual sponge-microbe-synsedimentary cement framework in a Late Ordovician reef, Southampton Island (Nunavut, Canada)

[1] Castagner, Ariane, [1] Desrochers, André, and [2] Lavoie, Denis

[1] Department of Earth and Environmental Sciences, University of Ottawa, Ottawa, Canada ON K1N 6N5 (acast097@uottawa.ca; andre.desrochers@uottawa.ca)

[2] Natural Resources Canada — Ressources Naturelles Canada, GSC-Quebec/CGC-Québec, 490, rue de la Couronne, Québec, Canada QC G1K 9A9 (denis.lavoie@canada.ca)

Abstract

A large, resistant buildup at the top of the Upper Ordovician (Hirnantian?) Red Head Rapids Formation (RHR) on Southampton Island (Nunavut, Arctic Canada) is dominated by massive boundstone and cementstone facies. These massive facies have more in common with the sponge–microbial reefs that dominated worldwide in the Early Ordovician, including the following primary components: early calcified sponge material, microbial elements, and synsedimentary cement. A close spatial relationship between sponge and microbial framework elements suggests that a poorly preserved decaying sponge framework provided substrates for the attachment and development of microbes, and that the microbes played essential roles as reef consolidators. Centimetre-scale colonial metazoans are present and locally intergrown with the sponge and microbial components. Other moind-dwelling invertebratesor calcareous algae are rare. Although altered now to calcite, cement fabrics suggest that aragonite was ubiquitous as sea-floor precipitate. Prior to its subaerial exposure in the latest Ordovician, the RHR buildup developed on the margin of a shallow-marine evaporative epicratonic basin where a diverse community of reef-building metazoans was unable to flourish.

Keywords: Upper Ordovician, Reefs, Carbonate Sedimentology, Carbonate Diagenesis, Arctic Canada

Introduction

Small and large Upper Ordovician buildups (Heywood and Sanford 1976; Bolton et al. 1977; Zhang 2010) have been reported from the Hudson Bay Basin on Southampton Island (Nunavut), Arctic Canada. These mounds consist of a relatively massive core with no obvious reef-building metazoans, raising the question of how much *in situ* biogenic material was involved. The massive cores have been loosely described in the past as algal or microbial limestones with calcareous metazoans of subsidiary importance. Here we present previously unreported biotic and abiotic components responsible for the mound growth and discuss how these components assemble to form reefal facies that are compositionally distinct from other coeval bioconstructions of the peri-Laurentian regions.

Geological context

The Hudson Bay Basin (Fig. 1) is a Phanerozoic intracratonic basin surrounded on all sides by Precambrian rocks of the Canadian Shield and dissected by "arches" (Sanford and Grant 1990, 1998; Hamblin 2008). To the south, the Cape Henrietta Maria Arch separates the Hudson Bay Basin from the smaller Moose River Basin whereas the Boothia-Bell Arch separates the Hudson Bay Basin from the smaller Foxe Basin of the Southeast Arctic Platform (Zhang 2010). The Paleozoic succession of the Hudson Bay Basin includes Upper Ordovician to Upper Devonian shallow-marine carbonate rocks, reefs, and shales, with locally thick Lower Devonian evaporite rocks. Paleozoic strata are unconformably overlain byerosional remnants of interpreted Mesozoic and Cenozoic non-marine and marine strata (Sanford and Grant 1998).

The onshore northern segment of the Hudson Bay Basin is well exposed in our study area located on Southampton Island, southern Nunavut (Fig. 1). The succession includes, in ascending order, the Upper Ordovician Bad Cache Rapids and Churchill River groups and Red Head Rapids Formation, and Lower Silurian Severn River, Ekwan River and Attawapiskat formations (Sanford and Grant 1998). The upper Katian (upper Richmondian) Red Head Rapids (RHR) Formation conformably overlies the upper Katian (lower Richmondian) Churchill River Group.

The former formation is divided into four units and capped by thin-bedded dolomitic limestone with local bioherms up to 400 m in diameter and 8 m in thickness (Zhang 2008). The massive bioherm cores have been loosely described in the past as algal or microbial limestones with calcareous metazoans of subsidiary importance (Heywood and Sanford 1976; Zhang 2010). These bioherms may have excellent potential as reservoir facies judging by their porous nature (up to 15% by visual estimation) and stratigraphic position immediately above oil shale units (RHR unit 1 of Zhang 2010), although the timing of pore space evolution with respect to hydrocarbon generation and expulsion remains elusive (Lavoie et al. 2015). A major disconformity is present between the Upper Ordovician (upper Katian-Hirnantian?) RHR Formation and the overlying Lower Silurian Severn River Formation corresponding to the widespread Tippecanoe I-II disconformity, which is present over most of the interior sedimentary craton of Laurentia (Sloss 1988). This disconformity represents the O-S boundary interval in the study area; thus a depositional hiatus that corresponds to the Hirnantian/Gamachian (Zhang 2011). The presence of Hirnantian/ Gamachian strata in the youngest reefal unit 4 of the RHR Formation is not excluded, but remains equivocal in the absence of key conodont species (Zhang 2011). In the more central offshore Hudson Bay Basin, the RHR Formation consists of a mixed succession of anhydrite and minor gypsum beds, limestone, dolostone, and organic-rich shale capped by halite (Hu et al. 2011). In spite of its location within 10° of the paleoequator during the Late Ordovician, the study area was under relatively warm and arid conditions leading to the formation of intracratonic platform evaporite deposits. This area was also located along a pan-Laurentian equatorial, hurricane-free climatic belt (Jin et al. 2013).

Methods

The study area is located 34 km SW of Coral Harbour on Southampton Island (64 2’34.8”N; 83 49’33.60”W”) and briefly described as locality #13 in Zhang (2010), where a large, resistant mound at the interpreted top of the RHR Formation has been exhumed by recent erosion. The mound core facies is well exposed, but flanking and interreef facies are absent. The massive mound core is 400 m long (NW-SE direction) and 250 m wide in plan view and 10 m thick in

vertical section. In total, 87 hand samples were collected in 0.5 m vertical increment at six representative sections located around the exhumed core. Samples containing calcite were thin-sectioned, polished, and stained with Alizarin red S and potassium ferricyanide (Dickson 1966). Ourtransmitted light and cathodoluminescence (CL) microscopic observations focus on the identification of the biotic and abiotic primary components of the mound core rather than its diagenesis and pososity evolution; the latter will be presented later in a separate contribution. Biotic and abiotic primary components were also sampled for $\delta^{13}C$ and $\delta^{18}O$ analysis. Nine fresh, polished slabs were microdrilled to generate powder. Analyses were performed with a Gas Bench II interfaced with a Finnigan Mat Delta XL mass spectrometer at the G.G. Hatch Laboratory, University of Ottawa. Data are reported as $\delta^{13}C$ and $\delta^{18}O$ in permil (‰) with respect to the Vienna Pee Dee Belemnite, or VPDB standard. The analytical precision is ±0.1 ‰.

Microfacies description and interpretation

In outcrop, the studied RHR mound core rocks largely form a massive limestone facies (> 90% in total), but thin-bedded dolostones are locally present (Fig. 2 and Fig. 3A). The macrofauna is rare with only sparse tabulate corals. In hand specimen, most limestone samples display a distinctive megascopic clotted fabric in which small constructional cavities filled by calcite cement are present. In thin-section (Fig. 2), microfacies consist mainly of boundstone and cementstone containing the following components in order of importance: early calcified sponge material (see below), microbial elements, and synsedimentary cement. Centimetre-scale colonial metazoans (mainly tabulate and rugose corals) are present in growth position and locally intergrown with the sponge and microbial components. The role played by these colonial metazoans during the growth of this buildup is difficult to assess because they appear more diagenetically altered than the other primary components (see below). The spatial distribution of *in situ* sponge and metazoan components (Fig. 2), however, suggests that they were in competition as initial reef builders. Other invertebrates associated with these reefal limestones are ostracods and sparse cephalopod skeletons. Depositional lime mud (micrite) is also rare.

The sponge component in the boundstone displays a complex centimetre-scale maze-like structure formed by a mosaic of large, inclusion-rich, non-ferroan, non luminescent calcite crystals (Fig. 3B) with only vague preservation of an original spicular network. These calcite crystals are irregular to equant, non-drusy, and pseudopleochroic (Figs 3E and F). These yellow calcite crystals are neomorphic calcite after replacement of interpreted aragonite material. Similar crystal fabrics in a calcitized cephalopod skeleton also support this interpretation. The precipitation of aragonite crystals in decaying modern sponges is well documented (Neuweiler et al. 2007).

The microbial components commonly encrusted or bound the sponge material, partly to completely filling small growth cavities (Fig. 3B). These interpreted microbial components comprise laminated peloidal to centimetre-scale micritic bush-like fabrics (Fig. 3C), but *Epiphyton*-and *Renalcis*-like forms are also present. The latter grew upward and downward in centimetre-scale growth cavities and are encapsulated by synsedimentary cement (see below). This close spatial relationship suggests that sponges provided substrates for the attachment and development of microbes, and that the microbes played essential roles as consolidators, by encrusting reef-building sponges, a relationship seen in many early Paleozoic reefs (Adachi et al. 2011).

The synsedimentary cement is inclusion-rich, non-ferroan, non-luminescent calcite crystals (Figs 3B and 3D) filling small growth cavities, but also forming unconfined sea-floor precipitates. These calcite crystals are irregular to acicular, locally forming splays or fan-like arrangements of outward-spreading calcite crystals (Fig. 3F). The latter features are either isolated, or coalesced to form larger structures. This cement contains numerous discontinuous surfaces marked by the development of peloidal or micritic encrustations interpreted as microbial during brief pauses in cementation. Square crystal termini are locally present (Fig. 3D). All of the above petrographic evidence suggests neomorphic replacement of aragonite marine cement.

An important post-sedimentary product is a mixture of small, irregular, interconnected vugs produced by carbonate dissolution cutting across the original rock fabric. These vugs, as well as the primary pores, are either totally or partly filled by clear, blocky, non-ferroan calcite cement (Fig. 3E). The interpretation of these late diagenetic elements is beyond the scope of the present study and will be addressed in a separate contribution.

Stable isotope geochemistry

The oxygen and carbon stable isotope signature of the three main synsedimentary mound components is the following (Fig. 4): i) interpreted sponge material consisting of the neomorphic calcite crystals ($\delta^{13}C_{VPDB}$ ranging from 2.9 to 3.1; $\delta^{18}O_{VPDB}$ranging from -3.4 to -6.7); ii) interpreted microbial structures ($\delta^{13}C_{VPDB}$ ranging from 2.4 to 4.1; $\delta^{18}O_{VPDB}$ ranging from -3.7 to -7.1), and iii) interpreted synsedimentary cement ($\delta^{13}C_{VPDB}$ ranging from 2.7 to 2.8; $\delta^{18}O_{VPDB}$ ranging from -5.3 to -7.4).

Discussion

Any depositional interpretation of the RHR buildup on Southampton Island must take into account the following constraints: i) scarce epifaunal metazoan biota, ii) sparse depositional lime mud, iii) abundant aragonite precipitation occurring either as synsedimentary sea-floor cement or early replacement in decaying sponges, and iv) unusually high proportions of sponge, microbe, and synsedimentary cement together with some small colonial metazoans as the main reef-building components. A topic open for discussion at this stage concerns the isotopic signatures of the various primary buildup components encoded at time of the deposition during the Late Ordovician, but most likely modified by meteoric and burial diagenesis.

An unconformity, controlled by a global end-Ordovician glacio-eustatic sea level fall, marks the Ordovician–Silurian boundary in the Hudson Bay Basin (Pinet et al. 2013) and caps the RHR mound at the study site. This sea-level drawdown resulted in restricted basin circulation

and precipitation of the basin centre subaqueous evaporites, both sulphate and halite (Hu et al. 2011). Thus, during the late Ordovician, the Hudson Bay Basin, at equatorial paleolatitudes (Jin et al. 2013), was a region of sedimentation under evaporative conditions. Prior to their subaerial exposure, the RHR buildups, occupying a basin-margin position, grew in an overall hot and arid climate, spatially disconnected from the open seaway to the northeast (Sanford 1987). This shallow-marine evaporative epicratonic setting was unfavourable for most marine biota, which can tolerate seawater of 30–40‰ salinity only (James and Jones 2015), thus explaining the almost total absence of diverse and abundant invertebrates and calcareous algae as reef dwellers. The production of lime mud resulting today from the disintegration of algae and invertebrate skeletons (James and Jones 2015) was greatly reduced in the Hudson Bay Basin during the latest Ordovician. Although calcite precipitation and dissolution of biogenic aragonite are expected in shallow Ordovician calcite seas (Stanley and Hardie 1998), precipitation of sulphates removed Ca from seawater and raised the Mg:Ca ratio promoting aragonite precipitation as synsedimentary cement or early marine replacement of decaying sponge tissues in addition to the more typical calcite marine cement.

The Upper Ordovician RHR reefs are sponge-microbial-synsedimentary cement buildups with an uncommon epifaunal metazoan biota and do not resemble peri-Laurentian reefs of similar age. Metre-sized shallow-water and larger deeper-water stromatolitic mud-mounds associated with a relatively diverse epifaunal metazoan biota are known from Upper Ordovician carbonate successions in northern Greenland (Harper et al. 2014). Other Upper Ordovician peri-Laurentian reefs (Mackenzie Mountains, Anticosti Island) include skeletal-calcimicrobial mounds that were built by relatively small stromatoporoids and corals, bryozoans and calcimicrobes also associated with a diverse epifaunal metazoan biota (Cecile and Potter 1989; Copper 2001). These peri-Laurentian reefs are examples of the most dramatic event in Ordovician reef development, which occurred across the Middle-Late Ordovician boundary with the changeover from microbe-dominated to metazoan- and algae-dominated reef growth (Webby 2002). Thus, the Upper Ordovician RHR buildups have a composition more in common with the sponge–microbial reefs that dominated worldwide in the Early Ordovician. The sponges provided substrates for the attachment and growth of microbes, and the microbes and

synsedimentary cement played essential roles as consolidators, by encrusting and cementing reef-building sponges. Additionally, the sponges were susceptible to degradation via early diagenetic processes, and were preserved as a mosaic of neomorphic calcite crystals preserving a faint spicular network. Metazoan components were localized with a limited framebuilding role.

The primary building components of the RHR reefs have roughly the same $\delta^{13}C_{VPDB}$ values, but their $\delta^{18}O_{VPDB}$ values are more variable (Fig. 4). The $\delta^{13}C_{VPDB}$ values from carbonate rocks are typically less affected by diagenetic changes than $\delta^{18}O_{VPDB}$ values because in many cases the system is more or less rock-buffered for carbon and the pore fluids contain little carbon able to change the isotopic composition of the rock (Banner and Hanson 1990). In addition, prior to the radiation of land plants in the Silurian and Devonian, the relative absence of terrestrially derived organic matter during meteoric diagenesis helped the preservation of a near-pristine marine $\delta^{13}C$ record below subaerial surfaces (Given and Lohmann 1985; Jones et al. 2015). Unlike the oxygen isotopes, the $\delta^{13}C_{VPDB}$ values ofthe primary RHR mound components have preserved much their original geochemical signature. Their $\delta^{13}C_{VPDB}$ values are clearly enriched (Fig. 3) when compared to values for global marine calcite during the Katian based on analyses of well-preserved brachiopods (Shields et al. 2003). This enrichment, recording a drastic change from the assumed $\delta^{13}C_{VPDB}$ of the DIC values of the Katian open seawater, probably resulted from the increased restriction of the Hudson Bay Basin marking the first step in the sequence of events that eventually led to the deposition of the RHR deeper-basin evaporites. An alternative explanation is that these enriched $\delta^{13}C_{VPDB}$ values could have preserved a Hirnantian seawater signature (Fig. 3) because they occur within the range defined by well-preserved Hirnantian brachiopods (Shields et al. 2003; Fig. 3). Similar enriched $\delta^{13}C_{VPDB}$ values in the southern Hudson Bay Basin and adjacent Moose River Basin (Demski et al. 2015; Turner and Armstrong 2015) have been used to claim that the Hirnantian deposition was far more widespread on the Laurentian craton that realized previously. Further chemostratigraphic and biostratigraphic studies are, however, needed to evaluate if either a late Katian or Hirnantian age can be assigned to the RHR mound strata exposed on Southampton Island. Regardless of age, the reef-building consortium (i.e. sponges and microbes) of the RHR mound fundamentally differs from other shallow-water Hirnantian reefs that developed only in a

few sites and retained diverse biotas (Webby 2012). Thus, it is difficult to invoke here the collapse of the reef ecosystems after the Hirnantian mass extinction (Sheehan and Li and Kershaw 2003; Harris 2004) as the main driver. The unusual biological framework present in the RHR mound probably grew on the margin of a restricted, hypersaline basin where a diverse community of reef-building metazoans was unable to flourish.

Conclusions

1- An Upper Ordovician (late Katian-Hirnantian?) reef buildup exposed at the top of the Red Head Rapids Formation on Southampton Island (Nunavut, Arctic Canada) developed on the margin of a shallow-marine evaporative epicratonic basin where physical and chemical seawater parameters were distinct from the open ocean and where a diverse community of reef-building metazoans was unable to flourish.

2- The massive core of this buildup displays mainly boundstone and cementstone microfacies, with abundant early calcified sponge material, microbial structures, and synsedimentary cement. Other than centimetre-scale colonial metazoans locally intergrown with the sponge and microbial components, epifaunal invertebrates or calcareous algae are sparse.

3- The accretionary mechanisms of the RHR buildup were mainly the results of frame-building and binding by early-calcified sponges and microbial elements for the boundstone facies, and of marine cement precipitation near the sea floor for the cementstone facies.

4- The biotic composition of the Upper Ordovician RHR mound have more in common with those present in the sponge–microbial reefs that dominated worldwide in the Early Ordovician.

Acknowledgements

The authors thank the financial and logistical support of the Geomapping for Energy and Minerals Program (Phase 2) of Natural Resources Canada. AD acknowledges the support of the Natural Science and Engineering Council of Canada (Discovery Grant). We also thank Guest

Editor Michael J. Melchin, and Jisuo Jin and Elizabeth C. Turner for their helpful and thorough reviews of the manuscript. This paper is a Geological Survey of Canada contribution. It is also a contribution to the IGCP project 591 (The Early to Middle Paleozoic Revolution).

References

Adachi N., Ezaki, Y., and Liu, J. 2011. Early Ordovician shift in reef construction from microbial to metazoan reefs. Palaios, **26**:106–114.

Banner, J.L. and Hanson, G.N. 1990. Calculation of simultaneous isotopic and trace element variations during water-rock interaction with applications to carbonate diagenesis. Geochim. Cosmochim. Acta: **54**, 3123-3137.

Bolton, T.E., Sanford, B.V., Copeland, M.J., Barnes, C.R., and Rigby, J.K., 1977. Geology of Ordovician rocks, Melville Peninsula and region, southeastern District of Franklin. Geological Survey of Canada, Bulletin **269**: 134 p.

Cecile, M.P., and Potter, A.W. 1989. Upper Ordovician-Lower Silurian Misty Creek mounds, Mackenzie Mountains, N.W.T. Canadian Society of Petroleum Geologists, Memoir **13**: 177-182.

Copper, P. 2001. Reefs during the multiple crises towards the Ordovician-Silurian boundary: Anticosti Island, eastern Canada, and worldwide. Canadian Journal of Earth Sciences, **38**: 153-171.

Demski, M. W., Wheadon, B., Stewart, L. A., Elias, R. J., Young, G. A., Nowlan, G. S. and Dobrzanski, E. 2015. Hirnantian strata identified in major intracratonic basins of central North America: implications for uppermost Ordovician stratigraphy; Canadian Journal of Earth Sciences: **52**, 68-76.

Dickson, J.A.D. 1966. Carbonate identification and genesis as revealed by staining. Journal of Sedimentary Petrology, **36**: 491-505.

Given, R.K., and Lohmann, K.C. 1985. Derivation of the original isotopic composition of Permian marine cements. Journal of Sedimentary Petrology, **55**: 430-439.

Hamblin, A.P. 2008. Hydrocarbon Potential of the Paleozoic succession of Hudson Bay/James Bay: Preliminary conceptual synthesis of background data. Geological Survey of Canada, Open file **5371**: 1-12.

Harper, D.A.T., Jin, J. and Rasmussen, C.M.Ø. 2014. Late Ordovician carbonate mounds from North Greenland: a periLaurentian dimension to the Boda Event?. GFF, **136**: 95–99.

Heywood, W.W., and Sanford, B.V. 1976. Geology of Southampton, Coats and Mansel Islands, District of Keewatin, Northwest Territories. Geological Survey of Canada, Memoir **382**: 35p.

Hu, K., Dietrich, J., Dewing, K., Zhang, S., Asselin, E., Pinet, N., and Lavoie, D. 2011. Stratigraphic Correlations for Five Offshore Wells in the Hudson Bay Basin, Northern Canada. Geological Survey of Canada, Open File, **7031**. http://dx.doi.org/10.4095/289545

James, N.P., and Jones, B. 2015. Origin of Carbonate Sedimentary Rocks. Wiley, Oxford, UK. 464 p.

Jin, Jisuo, Harper D.A.T., Cocks, Robin M., McCausland, Phil J.A., Rasmussen, Christian M.Ø., and Sheehan, Peter M. 2013. Precisely locating the Ordovician equator in Laurentia. Geology **41**: 107-110.

Jones, D.S., Fike, D.A., Finnegan, S., Fischer, W.W., Schrag, D.P., and McCay, D. 2011.Terminal Ordovician carbon isotope stratigraphy and glacioeustatic sea-level change across Anticosti Island (Québec, Canada). Geological Society of America Bulletin,**123**: 1645-1664.

Lavoie, D., Pinet, N., Dietrich, J., and Chen, Z., 2015. The Paleozoic Hudson Bay Basin in northern Canada: New insights into hydrocarbon potential of a frontier intracratonic basin. Bulletin American Association of Petroleum Geologists, **99**: 859-888.

Li, Y. and Kershaw, S. 2003. Reef reconstruction after extinction events of the latest Ordovician in the Yangtzeplatform, South China. Facies, **48**: 269-284.

Neuweiler, F., Daoust, I., Bourque, P.A.., and Burdige, D.J. 2007. Degradative calcification of a modern siliceous sponge from the Great Bahama Bank, the Bahamas: a guide for interpretation of ancient sponge-bearing limestones. Journal of Sedimentary Research, **77**: 552-563.

Pinet, N., Lavoie, D., and Keating, P. 2013. Architecture and subsidence history of the Hudson Bay intracratonic basin. Earth Science Reviews, **125**: 1–23.

Sanford, B. V. 1987. Paleozoic geology of the Hudson Platform. Sedimentary Basins and Basin-Forming Mechanisms. Memoir **12**, p. 483-505.

Sanford, B. V., and Grant, A. C. 1990. New findings relating to the stratigraphy and structure of the Hudson Platform. Geological Survey of Canada, Paper **1990**: 17-30.

Sanford, B.V. and Grant, A.C. 1998. Paleozoic and Mesozoic geology of the Hudson and southeast Arctic Platforms. Geological Survey of Canada, Open File **3595**.

Sheehan, P. M. and Harris, M. 2003. Microbialite resurgence after the Late Ordovician extinction. Nature: **430**, 75-78.

Shields, G.A., Carden, G.A., Veizer, J., Meidla, T., Rong, J.-Y., and Li, R.-Y. 2003. Sr, C, and O isotope geochemistry of Ordovician brachiopods: a major isotopic event around the Middle-Late Ordovician transition. Geochimica et Cosmochimica Acta, **67**: 2005–2025.

Sloss, L.L., 1988. Tectonic Evolution of the Craton in Phanerozoic Time. In: Sloss, L.L. (Ed.), Sedimentary Cover — North America Craton. US. Geological Society of America, The Geology of North America, **D2**: 25–51.

Stanley, Steven M., and Hardie, Lawrence A.1998. Secular oscillations in the carbonate mineralogy of reef-building and sediment-producing organisms driven by tectonically forced shifts in seawater chemistry. Palaeogeography, Palaeoclimatology, Palaeoecology, **144**: 3-19

Turner, E.C., and Armstrong, D.K., 2015. Upper Ordovician stratigraphy of northern Ontario: differential subsidence and deposition in two late Ordovician basins contemporaneous with

Hirnantian glaciation and the Taconic orogeny. Ontario Geological Survey Open File Report **6313**, 32-1-32-22.

Webby, B.D. 2002. Patterns of Ordovician reef development. Society for Sedimentary Geology. Special Publication **72**:129-179.

Zhang, S. 2008. New insight into Ordovician oil shales in Hudson Bay: their number, stratigraphic position, and petroleum potential. Bulletin of Canadian Petroleum Geology, **56**: 300–324.

Zhang, S. 2010: Upper Ordovician Stratigraphy and Oil Shales on Southampton Island Field Trip Guidebook. Geological Survey of Canada, Open File **6668**, 42p.

Zhang, S. 2011. Late Ordovician conodont biostratigraphy and the age of oil shale intervals on Southampton Island. Canadian Journal of Earth Sciences. 48: 619-643.

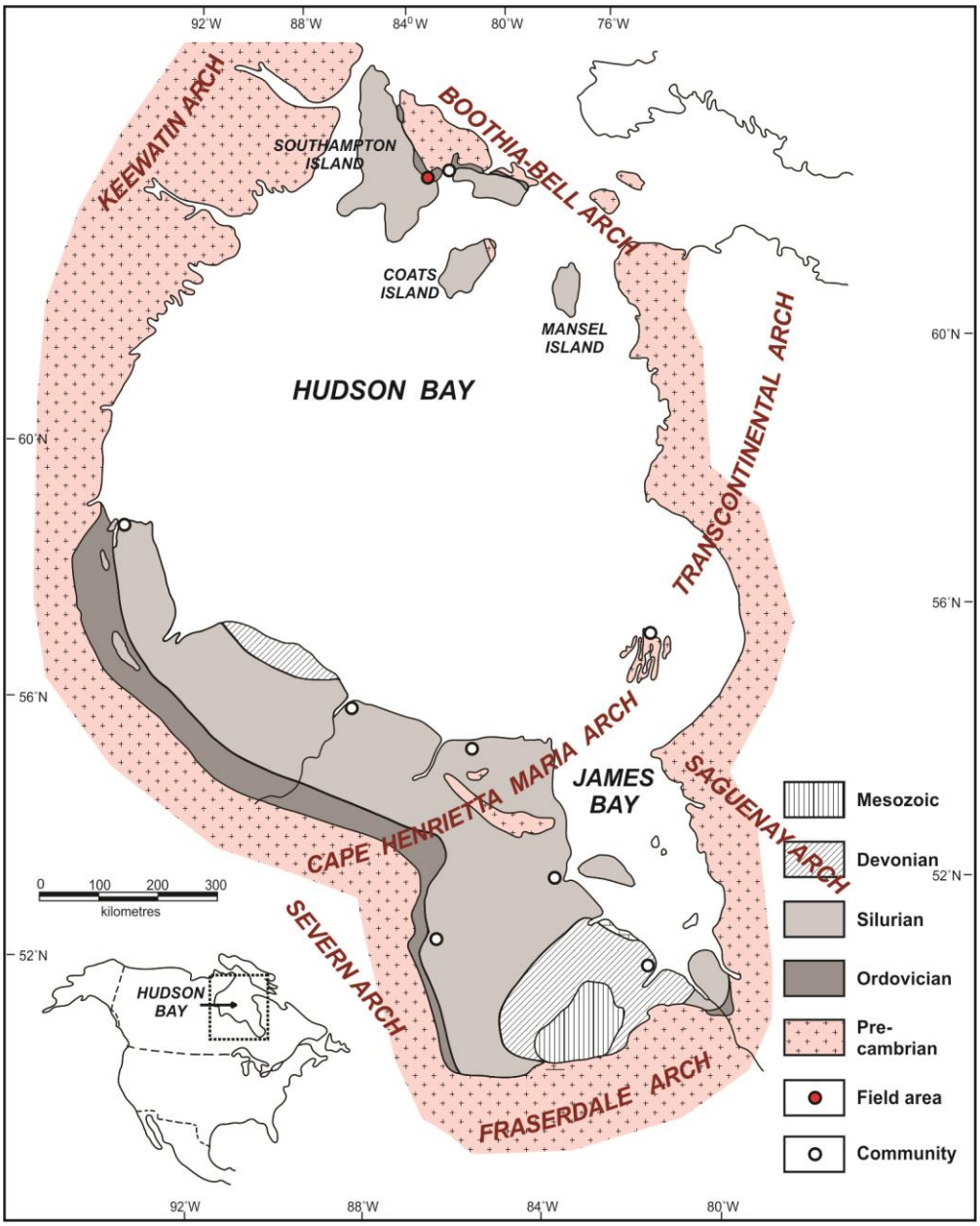
92°W
88°W
84°W
80°W
76°W
KEEWATIN ARCH
BOOTHIA-BELL ARCH
SOUTHAMPTON ISLAND
COATS ISLAND
MANSEL ISLAND
HUDSON BAY
TRANSCONTINENTAL ARCH
60°N
56°N
52°N
JAMES BAY
CAPE HENRIETTA MARIA ARCH
SAGUENAY ARCH
SEVERN ARCH
FRASERDALE ARCH
0 100 200 300
kilometres
HUDSON BAY
Mesozoic
Devonian
Silurian
Ordovician
Pre-cambrian
Field area
Community

Figure 1- Hudson Bay region, showing onshore Phanerozoic domains and general geological setting. The study area (red dot) is on Southampton Island. Figure modified from Zhang (2010).

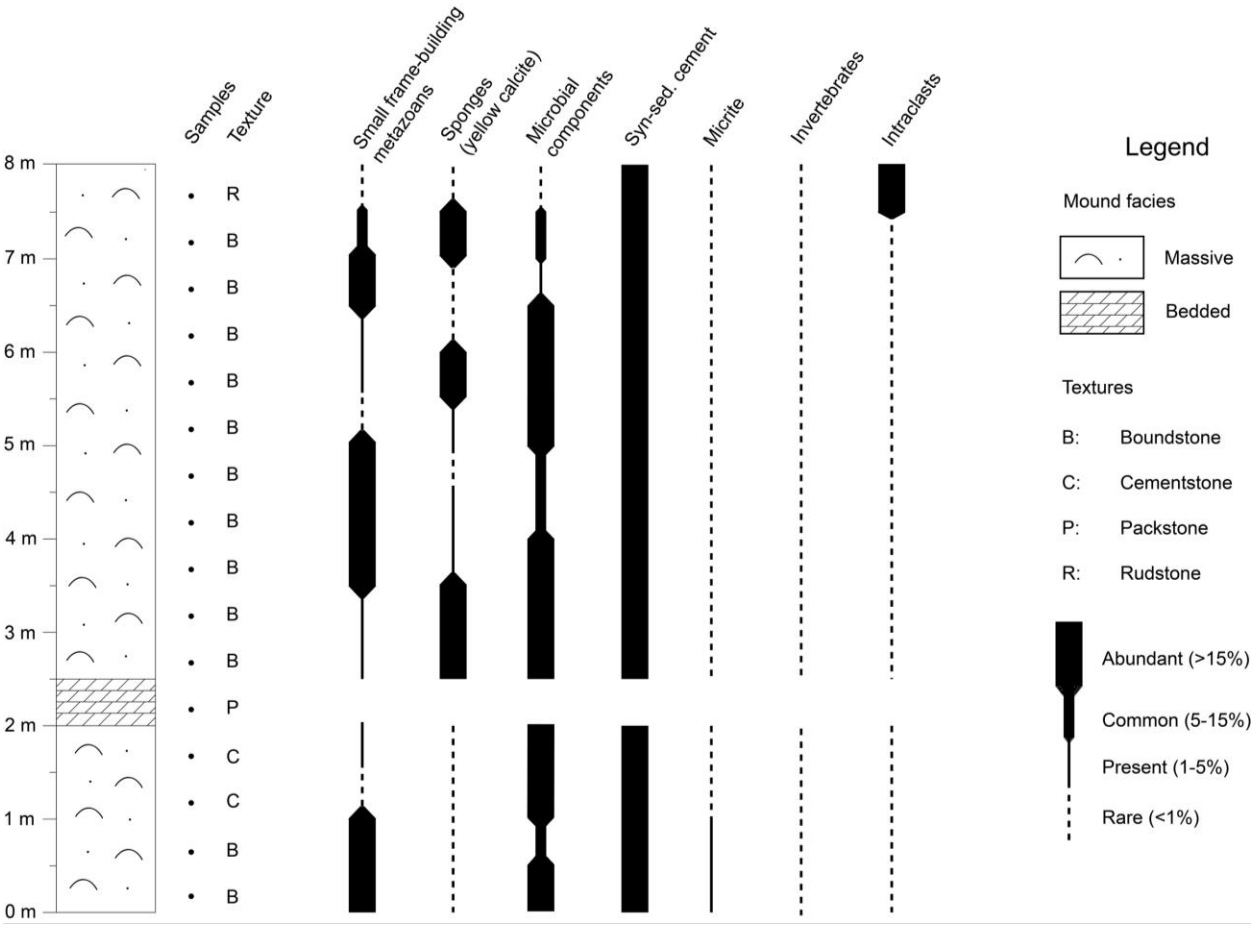

Figure 2- Upper Ordovician stratigraphy of the Southampton Island (Zhang 2011) with a representative stratigraphic section of the studied RHR buildup showing the mound attributes in the field (massive versus bedded facies) and the relative abundance of mound components in thin-section (metazoan, microbial elements, synsedimentary cement, micrite, and intraclasts). Please note that the contacts with the underlying RHR unit 3 and the overlying Lower Silurian Severn River Formation are not exposed in the study area (Zhang, 2010).

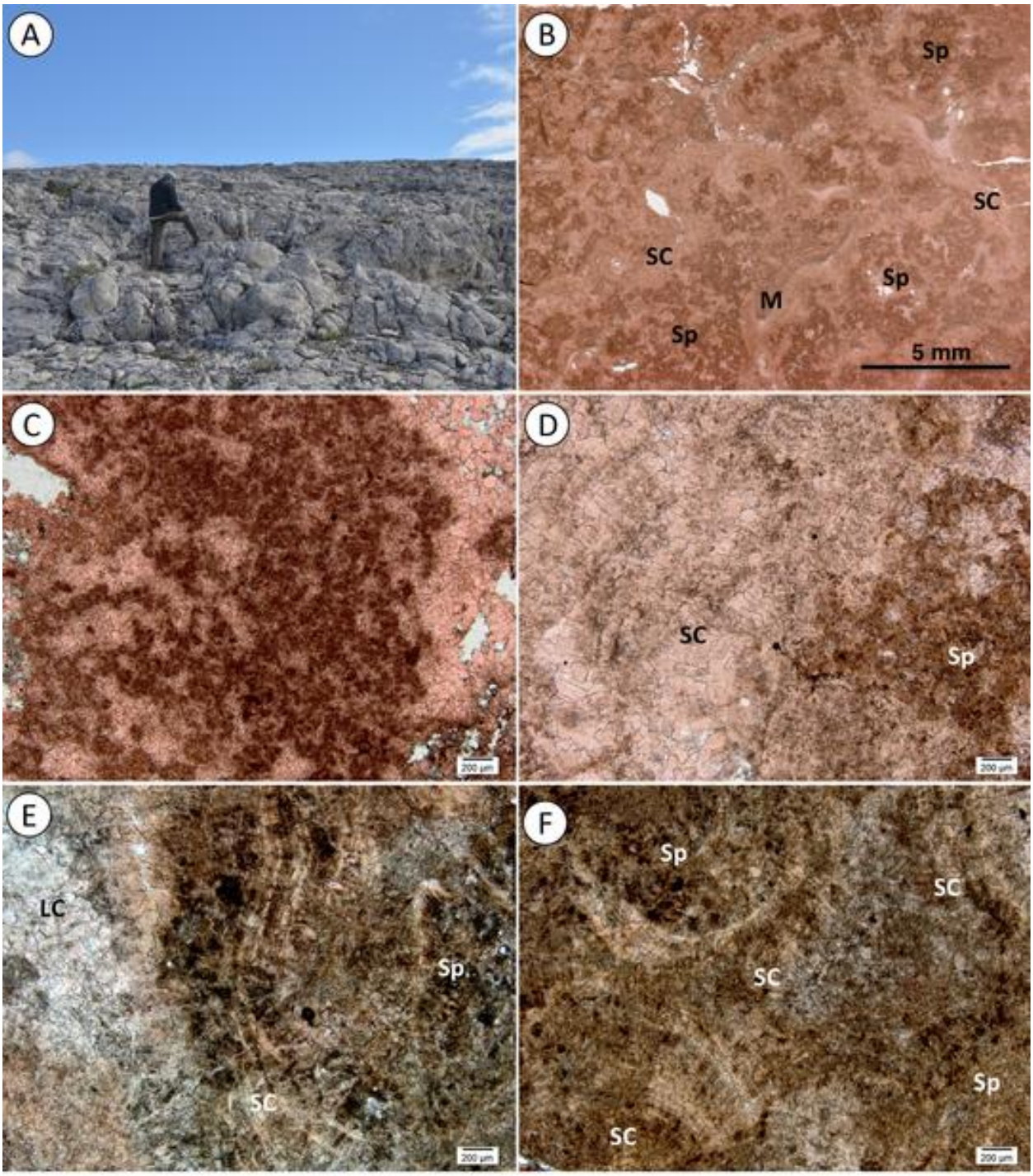
A
B
Sp
SC
SC
Sp
M
Sp
5 mm
C
D
SC
Sp
E
LC
Sp
SC
F
Sp
SC
SC
Sp
SC

Figure 3- A) Field photograph showing the massive nature and exposing about 6 m in thickness of the studied RHR buildup exposed on Southampton Island; B) Photomicrograph (boundstone microfacies) showing early calcified sponge material (Sp), microbial structure (M), and synsedimentary calcite cement (SC). Note the microbial structure (M) encrusting the roof of a small framework void; C) Photomicrograph illustrating a micritic microbial bush growing in a centimetre-scale growth cavity and encapsulated by synsedimentary cement; D) Photomicrograph (cementstone microfacies) showing inclusion-rich, non-ferroan, neomorphic calcite crystals (former aragonite seafloor precipitate; SC) filling a small growth cavity together with early calcified sponge material (Sp); E) Photomicrograph (boundstone microfacies) illustrating the infilling of a small growth cavity by early calcified sponge material (Sp), inclusion-rich synsedimentary cement (SC), and clear blocky calcite cement (LC); and F) Photomicrograph (cementstone microfacies) showing fan-like arrangements of acicular calcite crystals (SC).

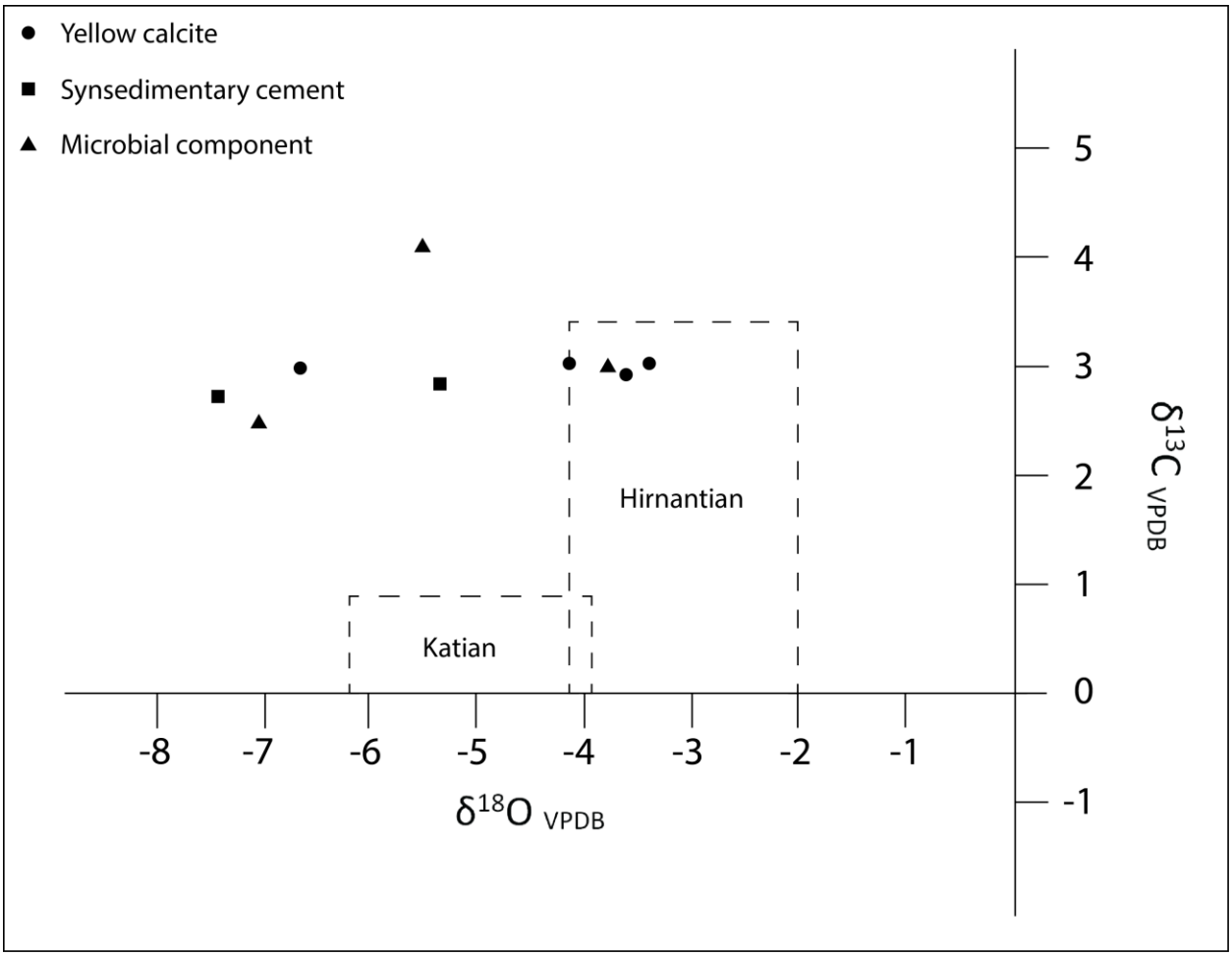

Figure 4- Cross-plot $\delta^{18}O_{VPDB}$ versus $\delta^{13}C_{VPDB}$ of the main primary components present in the RHR buildups. Variation in $\delta^{18}O_{VPDB}$ versus $\delta^{13}C_{VPDB}$ of Katian and Hirnantian Ordovician brachiopods is illustrated (data from Shields et al. 2003).